eLife

Reviewed Preprint
v1 • September 1, 2026
Not revised

For correspondence:
zqian@snnu.edu.cn
huixiao@snnu.edu.cn

Competing interests: No competing interests declared

Reviewing editor: Yihong Ye, National Institute of Diabetes and Digestive and Kidney Diseases, United States

Xkr regulates phosphatidylserine transport via ER-PM contact sites to promote apoptotic cell clearance

Qian Zheng, Xinyu Ma, Fuqiao Liu, Tong Xiao, Lei Yuan, Qing Yan, Hui Wang, Hui Xiao
College of Life Sciences, Shaanxi Normal University, Xi'an, China

eLife Assessment

This study presents **valuable** findings implicating Xkr and its newly identified binding partners in regulating the exposure of apoptotic signal for phagocytosis, suggesting that Xkr might facilitate phosphatidylserine transfer at the ER-plasma membrane contact sites. However, several conclusions, including caspase-independent activity of Xkr and its role at the ER-PM contact sites, are not well supported by experimental data. Furthermore, some key controls are missing, and in numerous places the authors' discussion has extended far beyond what the data support. The findings presented are currently **incomplete** and do not fully support key mechanistic claims of the study.

https://doi.org/10.7554/eLife.112294.1.sa3

Abstract:

Phosphatidylserine (PS) is an important apoptotic “eat me” signal for cell corpse clearance (efferocytosis). Phospholipid scramblase, such as Xkr8, allows PS exposure in a caspase-dependent manner. *Drosophila* Xkr, the Xkr8 homolog, lacks caspase recognition sites, implying an alternative efferocytosis pathway. Here, we show that Xkr directly interacts with *Drosophila* OSBP (dORP9), thereby enabling its localization to ER-plasma membrane (PM) contact sites. The deficiency of Xkr and dORP9 both leads to a severe reduction of PS exposure, and more cytoplasmic PS is retained in the endoplasmic reticulum, indicating that non-vesicular PS transport regulates apoptotic PS exposure and efferocytosis. Furthermore, Xkr accumulates at ER-PM contact sites after apoptosis, and the deficiency of *dorp9* disturbs this, disabling non-vesicular PS translocation to the PM. These results reveal a previously unrecognized function of the lipid scramblase Xkr as a PS transport channel via ER-PM contact sites, thereby mediating PS transport and exposure in efferocytosis.

Introduction

Billions of apoptotic cells are produced daily in multicellular organisms, which are efficiently removed by a highly conserved process called cell corpse clearance (efferocytosis) [1, 2]. Efferocytosis is essential for development, tissue homeostasis, and mitigation of inflammatory responses under physiological conditions [3], and depends on recognition of specific surface ligands, termed “eat me” signals, that distinguish apoptotic from healthy cells [4]. Phosphatidylserine (PS), the most well-known and conserved “eat me” signal, is exposed on the outer surface of apoptotic cells and binds to macrophage PS receptors to trigger engulfment of apoptotic cells [5]. In healthy cells, PS primarily localizes to the inner surface rather than the outer surface of the PM [6], and the exposure of PS on the cell surface results from scramblase activation. Apoptosis signals induce caspase-mediated cleavage of scramblases, especially Xkr8, allowing apoptotic PS externalization from the inner to outer PM leaflets to initiate efferocytosis [6]. The ubiquitously expressed Xkr8 localizes to the PM through heterodimerization and chaperoning by two type I membrane proteins, Basigin (BSG) and Neuroplastin (NPTN), which form a complex following caspase cleavage to promote apoptotic PS exposure [7]. Xkr8 deficiency

has been linked to systemic lupus erythematosus (SLE)-type autoimmune diseases and male infertility[8]. However, whether Xkr8 associates with other proteins to regulate PS exposure during apoptosis remains unclear.

PS is mainly synthesized in the endoplasmic reticulum (ER) and therefore requires transport to other membrane-bound cellular compartments [9]. Lipids can be transferred from the ER to other organelles via vesicular transport along the secretory and endocytic pathways [10, 11]. However, such transport alone cannot account for the compositional heterogeneity of different membranes. Mounting evidence suggests that non-vesicular transport provides an alternative, faster transport mechanism, particularly for the PM, which rapidly changes composition in response to cellular status [6, 12, 13]. Non-vesicular transport of PS from ER to PM is mediated by oxysterol-binding protein (OSBP) and OSBP-related proteins (ORPs) located at ER-PM contact sites, which recruit various protein players to promote lipid exchange between ER and PM, which is essential for many physiological processes [14, 15]. In particular, ORP5 and ORP8 have recently been shown to mediate countertransport of phosphatidylinositol 4- phosphate (PI4P) and PS between the ER and PM, transferring PS from the ER to the PM in concert with PI4P from the PM to the ER, in a PI4P gradient-dependent manner. Importantly, PI4P delivered to the ER is immediately dephosphorylated by the ER- resident phosphatase, suppressor of actin mutations 1-like (Sac1), to maintain an extremely low PI4P gradient level in the ER [16].

In *Drosophila melanogaster*, apoptotic cells are removed during efferocytosis by nonprofessional phagocytes (e.g., epithelial cells) or professional phagocytes (i.e., macrophages and glial cells), thereby exposing PS and recruiting Drosophila macrophages via a mechanism similar to that in mammals [17]. In *Drosophila*, PS is exposed on the surface of degenerating or pruned neurons and recognized by receptors on the surface of phagocytes, such as Draper and SIMU [18, 19], thereby mediating the clearance of neuronal fragments. Meanwhile, some bridging molecules, such as Onion and NimB1, also positively or negatively regulate the recognition and phagocytosis of apoptotic cells via binding to PS [20, 21]. Exposed PS can be detected on the cell surface of damaged or apoptotic cells in flies, indicating that PS exposure is specifically regulated by apoptotic signals and is crucial for subsequent efferocytosis [22–24]. Because the *Drosophila* homolog of Xkr8, Xkr, was considered to lack a caspase recognition site compared with the mouse Xkr8 and *C. elegans* CED-8 amino acid sequences [25], this has raised a long-standing question as to whether Xkr regulates PS exposure as a phospholipid scramblase during apoptosis in *Drosophila*. However, a recent study showed that Xkr can be constitutively activated to disrupt the asymmetric distribution of phospholipids, thereby altering the deformability of cell membranes [26], suggesting that Xkr may have participated in apoptotic PS exposure or the following efferocytosis.

In this study, we confirmed that Xkr exhibited scramblase activity to mediate PS exposure during apoptosis; Xkr deficiency led to a significant reduction in PS exposure and efferocytosis both in *Drosophila* S2 cells and embryos. Through mass spectrometry screening and immunoprecipitation, we identified the transmembrane protein, TM9SF4, and the ER phospholipase Sac1, which regulated the PS distribution; disordered PS distribution also caused reduced PS exposure and inefficient efferocytosis. Additionally, we found that the *Drosophila* ORP, dORP9 (CG1513), directly interacted with Xkr via its pleckstrin homology domain, regulating apoptotic PS exposure in *Drosophila* S2 cells, while Xkr accumulated specifically at ER-PM junctions. Our results demonstrated that Xkr cooperated with dORP9 to mediate non-vesicular PS transport, thus exhibiting PS externalization to mediate efferocytosis in flies. Our work uncovers a new caspase-independent apoptosis response mechanism mediated by the phospholipid scramblase Xkr, which regulates non-vesicular PS transport from the ER to the PM, responsible for efficient PS exposure and apoptotic cell clearance conserved from insects to mammals.

Results

Xkr exhibits scramblase activity, participating in PS exposure and apoptotic cell clearance *in vitro* and *in vivo*

Activation of Xkr8 in mammals and CED-8 in *Caenorhabditis elegans* both require a caspase-3 cleavage site to expose apoptotic PS. However, in *Drosophila*, Xkr lacks both N- and C-terminal domain caspase recognition motifs (Figure S1A) [27]. To investigate how Xkr mediates scramblase activity, we first expressed N- and C-terminal fusion reporters, GFP-Xkr and Xkr-GFP, in *Drosophila* S2 cells, wherein Xkr primarily localized to the plasma membrane with a lesser proportion also present in the cytoplasm (Figures 1A and 1B). To test whether Xkr could indeed expose PS during apoptosis, we treated S2 cells with *xkr*-RNAi or control-RNAi for staining with FITC-labeled annexin V before inducing apoptosis. Subsequent flow cytometry analysis showed that *xkr* knockdown significantly reduced the levels of exposed PS (Figure 1C).

To define the precise role of Xkr in PS exposure during apoptosis, we used CRISPR/Cas9 to generate a mutant S2 cell and mutant flies harboring an early translation termination codon in Xkr (Figures 1D and 1E). Xkr antibody immunofluorescence staining confirmed that wild-type (WT) Xkr primarily localized on the plasma membrane, whereas no Xkr signal was detected in xkr^{ko} S2 cells (Figure S1B). Flow cytometry analysis indicated that the ability of xkr^{ko} cells to expose PS on the outer plasma membrane was significantly reduced. At the same time, re-expression of Xkr in the mutant restored the PS exposure (Figure 1F), thus demonstrating that Xkr was important for apoptotic PS exposure in S2 cells. To further assess Xkr scramblase activity during apoptosis, WT and *xkr* mutant cells were treated with a fluorescently labeled phospholipid analog, NBD-PC, which was internalized after inducing apoptosis. NBD-PC levels on the inner leaflet were significantly lower in xkr^{ko} cells (Figure 1G), showing that scramblase activity was suppressed in the absence of functional Xkr. These results indicate that Xkr facilitates phospholipid scrambling in the plasma membrane and mediates PS exposure during apoptosis, thus supporting a conserved role of Xkr in PS exposure between insects and mammals. As apoptotic cells are recognized and cleared by macrophages in a PS-dependent manner, we hypothesized that loss of scramblase function in S2 cells could also impair the recognition and clearance of apoptotic cells (ACs). To test this possibility, we applied Cell Tracker™ Red CMTPX to label both WT and xkr^{ko} cells, induced apoptosis by exposing them to actinomycin D (AcD) for 1 h, and then added them to non-apoptotic WT S2 cells to initiate efferocytosis. Confocal microscopy showed that a single phagocyte contained approximately 3.8 CMTPX-labeled ACs in assays with apoptotic S2 cells as prey. In contrast, only 1.8 CMTPX-positive ACs were detected on average using xkr^{ko} cells as prey (Figures 1H and 1I, and figures S1C and S1D).

In *Drosophila* reared at 25°C, ACs begin to appear at stage 11 of embryogenesis[28], followed by macrophage engulfment originating in the cephalic mesoderm and spreading throughout the embryo. To further investigate the role of Xkr in cell corpse engulfment in *Drosophila*, we generated a xkr^{ko} fly line using CRISPR/Cas9 (Figures 1D and 1E). We confirmed the null allele mutant status by immunofluorescence staining (Figures S1E and S1F). We then employed the phagocytic index (PI), i.e., number of apoptotic particles per macrophage, to quantify macrophages' capacity to engulf apoptotic bodies [29, 30]. We found no significant differences in the number of macrophages at stage 13 between WT and xkr^{ko} flies (Figures 1J and 1K), indicating that the embryo development was unaffected by Xkr deletion. However, we observed a higher number of unengulfed ACs in the xkr^{ko} mutant. In comparison, the number of engulfed ACs per macrophage was approximately 50% lower in xkr^{ko} flies compared to that in WT (average ACs/macrophage: 1.6 vs 2.6, xkr^{ko} vs WT; Figures 1J to 1L). In *Drosophila*, the hemolectin (Hml) protein is specifically expressed in embryonic and larval hemocytes, particularly in plasmatocytes and crystal cells, making it a suitable marker for labeling macrophages [31]. To further confirm that Xkr-mediated PS exposure in apoptosis promoted macrophage recruitment and corpse recognition, we used an *Hml-GAL4* driven *UAS-GFP* (*Hml>GFP*) reporter fly strain for labeling macrophages. Fluorescence microscopy revealed that ACs in xkr^{ko} embryos were generally

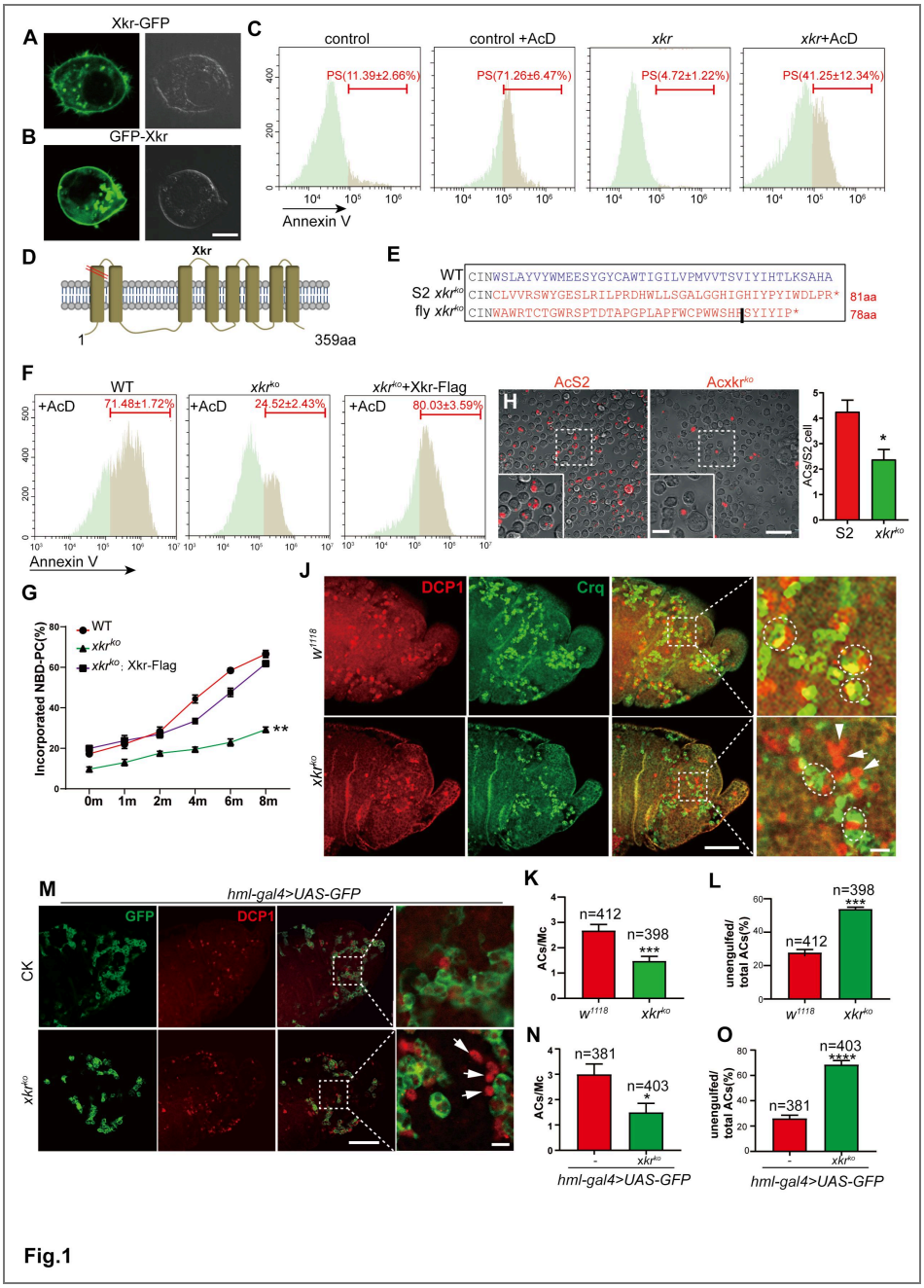

Fig.1

Figure 1. **Xkr cooperates with TM9SF4 and dORP9 to regulate efferocytosis in *Drosophila* embryos.**

unengulfed or found at low levels within macrophages. In contrast, the majority of ACs were engulfed by GFP-positive macrophages in control *Hml>GFP* embryos (Figures 1M to 1O). Taken together, these results demonstrated that Xkr-mediated PS exposure plays a prominent role in the recognition and clearance of ACs by macrophages.

TM9Sf4 is identified to interact with Xkr to regulate PS distribution for exposure in apoptosis

Since the above result indicates that Xkr regulates apoptotic PS exposure in a caspaseindependent manner, it remains unclear whether Xkr activity is specifically activated by apoptotic signals. We detected the mRNA and protein level of Xkr after apoptosis induction, and found that Xkr protein level increased after apoptosis induction, whereas *xkr* mRNA was unaffected (figures S2A to S2C). And, we conducted subcellular colocalization assays by expressing the Xkr-mCherry reporter in a panel of S2 cell lines with various GFP-labeled organelles. These assays revealed that Xkr could colocalize with, i.e., physically contact, membranous organelles such as endosomes or the ER (Figures S2D to S2H). To explore the function of cytoplasmic Xkr and its regulatory mechanism in efferocytosis, we performed immunoprecipitation-mass spectrometry proteomics (IP-MS) to screen the candidate proteins interacting with Xkr (Figure 2A), and identified 81 putative Xkr-interacting proteins (Data S1). Considering the properties and distribution of Xkr in cells, we selected the transmembrane 9 family protein, TM9SF4, which reportedly contributes to the regulation of innate immunity mediated by hemocyte phagocytosis in Drosophila, for closer examination [32] (Figure S3A). Subsequent Co-IP assays indicated that Xkr interacted with TM9SF4 in S2 cells (Figure 2B), and the co-expression of Xkr-GFP with TM9SF4-mCherry in S2 cells indicated that they mainly colocalized in the plasma membrane, with a proportion also co-localized in the cytoplasm (Figure 2C). Yeast two-hybrid (Y2H) assays and bimolecular fluorescence complementation (BiFC) assays in HEK 293T cells revealed that Xkr likely directly interacted with TM9SF4 (Figure 2D; figure S3B), suggesting that TM9SF4 may chaperone Xkr to the plasma membrane, which aligns with its reported role in other protein interactions[33].

TM9SF4 encodes a nonaspanin-type protein, which has been reported to be involved in cellular immunity and cell adhesion [34] in both humans and *Drosophila*. TM9SF4 is primarily localized to the Golgi apparatus and early endosomes and has been shown to directly interact with the phospholipase Sac1 [35]. We performed IP-MS of Flag-Sac1 in S2 cells and identified TM9SF4 as a candidate interacting protein (Figures S3C to S3E, Data S2). Subsequent Co-IP experiments and BiFC assay in HEK 293T cells further verified direct TM9SF4-Sac1 interaction (Figure 2E; figure S3F). Co-expression of TM9SF4-mCherry and Sac1-GFP in S2 cells showed that a proportion of intracellular TM9SF4-mCherry signals colocalized with Sac1-GFP puncta (Figure 2F). As a lipid phosphatase, Sac1 is known to dephosphorylate PI4P in the ER to maintain the lipid gradient and facilitate continuous PS delivery to the PM or other organelles [16]. Although Y2H assays showed that Sac1 did not directly interact with Xkr (figure S3H), silencing *tm9sf4* or *sac1* both resulted in a similar reduction in apoptotic PS exposure to xkr^{ko} (Figure 2G), indicating that the transport of phospholipids may play a role in PS exposure.

Based on our discovery of the interaction between Xkr and TM9SF4, we assessed whether TM9SF4 or Xkr affected the subcellular distribution of PS. As the C2 domain of lactadherin (Lact::C2) can specifically bind to the biologically relevant PS isomer, phosphatidyl-L-serine, and thus serve as a probe to label PS [36], we used a mCherry-Lact::C2 fusion reporter to visualize cellular PS in S2 cells [37]. Fluorescence microscopy analysis showed that mCherry-Lact::C2 was primarily localized in the PM, and to a significantly lower extent in cytoplasmic organelles, especially the ER, in S2 cells (Figure 2H). Subsequently, induction of apoptosis led to PS enrichment at the PM (Figure S3I). By contrast, PS levels were significantly lower at the cell membrane of xkr^{ko} cells compared to those in S2 cells (Figures 2H′ and 2I). In contrast, knockdown of either *tm9sf4* or *sac1* resulted in obviously reduced PS localization to the PM, but increased localization in intracellular membrane structures (Figures 2H′′ and 2H′′′). If Xkr deficiency disrupted PS transport, more PS would be retained in the ER. When we co-expressed PS indicator (mCherry-Lact::C2) and ER indicator (Calr-GFP), we observed greater signal overlap in xkr^{ko} cells (Figures 2J

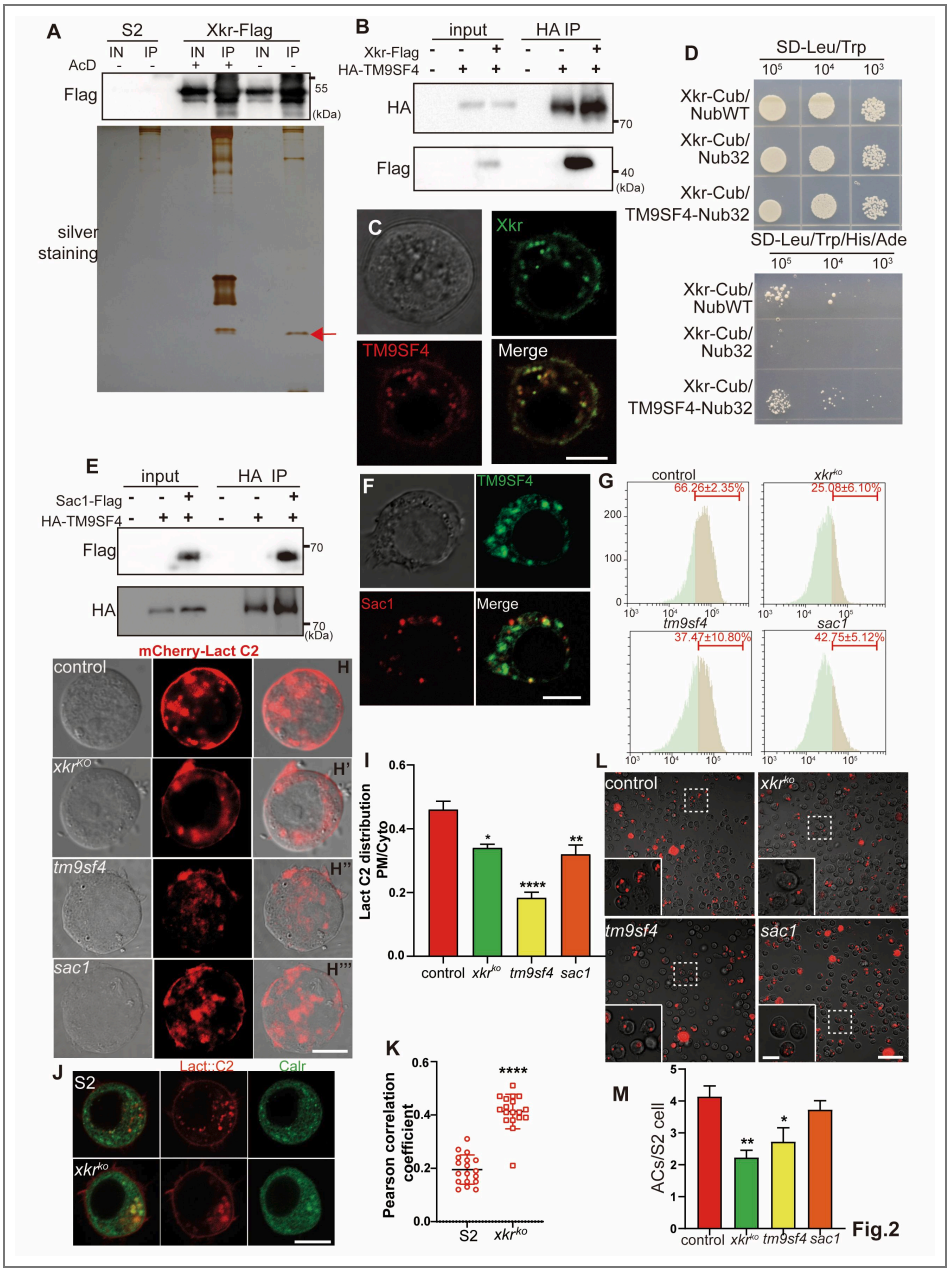

Figure 2. **Non-vesicle transport of PS from ER to PM participates in the exposure of apoptotic PS**

and 2K), indicating that Xkr regulated PS exposure via PS transport from the ER to the PM. Furthermore, this disrupted PS localization to the PM could not be restored by apoptosis induction (Figures S3I and S3J), indicating that apoptotic PS exposure depended on PS delivery from the ER to the PM. Sac1 has been reported to regulate PS transport by dephosphorylating PI4P on the ER, to establish a linkage mechanism for the opposite transport of PI4P and PS. Since *tm9sf4* and *sac1* knockdown both resulted in impaired PS exposure similar to that in xkr^{ko} cells, *sac1* RNAi in ACs only slightly declined efferocytosis with no significant difference (Figures 2L and 2M). Therefore, we assume that there is a more direct and efficient manner to facilitate apoptotic PS transport and efferocytosis.

Non-vesicular PS transport is required for apoptotic PS exposure and efferocytosis

As the above results revealed a role for Xkr in both distribution and translocation of PS at the PM, as well as in mediating apoptotic PS exposure, we next investigated whether components involved in non-vesicular PS transport might also participate in PS exposure during apoptosis. ORP5/ORP8 (oxysterol-binding protein (OSBP) - related protein, ORP) were located at membrane contact sites (MCS) between the ER and PM, which were recently shown to play a crucial role in regulating phosphatidylinositol 4- phosphate (PI4P) and PS levels in the PM [38]. Studies in yeast and human cells have shown that ORPs form MCSs between the ER and the PM, thus regulating lipid homeostasis via facilitating non-vesicular lipid exchange [37]. There are five ORPs in *Drosophila* (Figure 3A) with uncertain roles in PS transport at the MSCs between different organelles, while ORPs and its homologs are conserved between yeast (Osh family) to mammals (ORP family), and share a lipid binding domain (ORD) structure in the C-terminal region, and a pleckstrin homology (PH) domain in the N-terminal region with high affinity for PM-associated PI4P (Figure S4A) [37, 39]. The phylogenetic analysis of ORPs from yeast, *Drosophila,* mice, and humans (Figure S4B) resulted in the annotation of CG3860 as dORP2 and CG1513 as dORP9. Most *Drosophila* ORPs lack an ER transmembrane domain, suggesting that the ER integral membrane proteins may play more essential roles in recruiting *Drosophila* ORPs to the ER membrane. VAP (VAMP-associated protein, VAP33 in *Drosophila*) has been reported as an ER-anchored protein that interacts with various lipid transport proteins at ER-organelles MCSs [40].

Therefore, we generated knockdown S2 cell lines by RNAi for five *orp* genes, as well as *vap33*, to assess the role of ORPs in facilitating PS exposure during apoptosis. Annexin V-PS analysis by flow cytometry showed that *dOrp9*, *dOrp2*, or *cg9205* knockdown each resulted in significantly decreased PS exposure to 29.10%, 44.94%, and 31.18%, respectively, compared with 75.55% in RNAi non-targeted control cells. Additionally, *vap33* knockdown also inhibited apoptotic PS exposure (Figure 3B; figure S4C), indicating that PS transport via the PM-ER MCS promotes PS exposure in ACs. We then determined whether PS transport via PM-ER MCS was required for efferocytosis and found that silencing *tm9sf4*, *dorp2*, or *dorp9* could also reduce ACs recognition (Figures 3C and 3D), similar to xkr^{ko}. These results indicate that non-vesicular PS transport via the PM-ER MCS is essential for efferocytosis. Co-IP, Y2H, and BiFC assays indicated that Xkr likely directly interacts with both dORP2 and dORP9 (Figures 3E and 3F; figure S4D), and the co-localization of Xkr-GFP and mCherry-dORP2/mCherry-dORP9 in S2 cells showed that Xkr and dORP9 had more overlapping areas in cytoplasmic vesicles (Figure 3G; figure S4E). The endogenous Xkr can be immunoprecipitated by dORP9-Flag (figure S4F), which indicated that the interaction was not artificial or due to excessive protein expression. Meanwhile, we found that the cytoplasmic TM9SF4 also overlapped with dORP9 (figure S4G). To investigate whether knockdown of these genes affected apoptosis, we measured the levels of cleaved *Drosophila* Dcp-1(a caspase-3 homolog in *Drosophila*), which only recognizes endogenous levels of the cleaved Dcp-1 fragment during apoptosis. We found that Dcp-1 could be detected by adding actinomycin D to S2 cells, and neither xkr^{ko} nor *tm9sf4*, *sac1*, nor *dorp9* prevented apoptosis (Figure S4H). These results suggested that Xkr did not affect apoptosis, that the apoptosis signal induced Xkr levels without caspase activation, and that increased Xkr may accelerate non-vesicular PS transport for efficient apoptotic PS exposure.

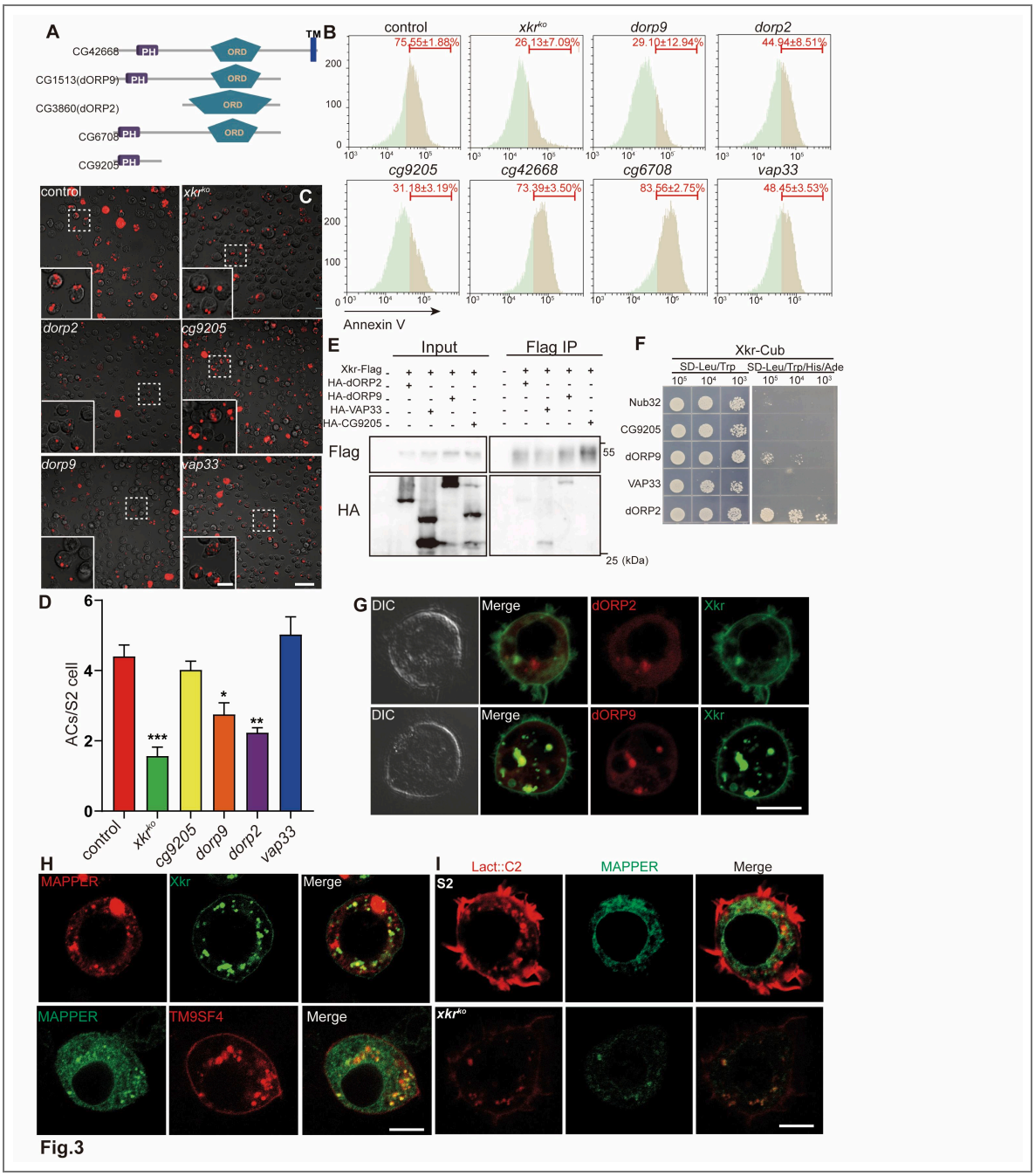

Fig.3

Figure 3. Schematic model for Xkr promoting PS exposure by accelerating PS transport via ER-PM contact sites.

To investigate whether Xkr and TM9SF4 transferred apoptotic PS via ER-PM MCS, we employed a GFP-MAPPER or mCherry-MAPPER construct to monitor ER-PM contact sites selectively. Co-localization of MAPPER and Calr indicated that MAPPER was appropriate for monitoring ER-PM MCS(figures S5A and S5B) [41]. Confocal microscopy of S2 cells co-expressing GFP-MAPPER with TM9SF4-mCherry, or mCherry-MAPPER with Xkr-GFP, revealed Xkr and TM9SF4 localization at the plasma membrane, with an intracellular proportion of the signal for each protein overlapping with MAPPER (Figure 3H). Furthermore, the induction of apoptosis increased ER-PM MCSs and the accumulation of Xkr at ER-PM MCSs (figure S5C), supporting the role of Xkr in regulating PS transport via ER-PM MCS during apoptosis. Co-expression of Lact::C2 with MAPPER in S2 and xkr^{ko} cells showed that PS levels were reduced in the PM of xkr^{ko} cells, while fewer ER-PM MCSs were detected in xkr^{ko} cells than in WT (Figure 3I). These results suggest that apoptotic PS exposure was driven by PS transport via PM-ER MCS.

dORP9 serves as a bridge that strengthens ER-PM MCS through interactions with Xkr and VAP33

Protein structure analysis on the Swiss-Model website revealed that both dORP2 and dORP9 lack an ER TM domain. Therefore, we hypothesized that OSBP requires VAP33 to maintain ER stability in *Drosophila*. Although VAP33 was immunoprecipitated with Xkr, no apparent direct interactions were observed between them in Y2H assays. Further Co-IP analysis of possible VAP33 interactions with dORP9/dORP2, followed by BiFC experiments, indicated that VAP33 could directly interact with dORP2 and dORP9 (Figures S5D and S5E). dORP2 lacks the PH domain, and Xkr showed a more overlapping expression region with dORP9; meanwhile, the interaction between Xkr and dORP9 was enhanced after apoptosis induction, whereas inhibiting apoptosis significantly reduced the interaction (Figure S5F). We hypothesized that the interaction between Xkr and dORP9 was more specific to apoptosis. Structural analysis of dORP9 identified a PH domain that reportedly binds PI4P and an ORD domain that functions in lipid transport (Figure 4A) [39]. To narrow down the scope of regions potentially required for the dORP9-Xkr interaction, we generated a series of dORP9 truncation variants. Co-IP, Y2H, and BiFC assays indicated slight differences in the interacting domains between Xkr and dORP9, whereas all assays supported the direct interaction between Xkr and the dORP9 PH domain (Figures 4B to 4D). To enhance persuasiveness, we used Alphafold3 to predict binding sites through structural analysis, and the computational model confirmed that the intracellular loop of Xkr (D298, T301, E304, Y305, between the 6th and 7th transmembrane domains) substantially bound to the dORP9 PH domain (1-150AA) (Figure 4E). Similarly, the FFAT (diphenylalanine in an acidic tract, EFFDAxE) motif of ORP proteins can bind to the ER anchoring protein VAP, connecting OSBP to the ER membrane and mediating its structural role in supporting ER-PM MCSs [11]. Co-IP, Y2H, and BiFC assays demonstrated that the dORP9 FFAT motif (EEDFYDAYDD) likely shared direct interactions with VAP33 (Figures 4F to 4H), and Alphafold3 calculated that dORP9 likely interacts with VAP33 via the FFAT-interacting domain (Y310, D311, A312, Y313, D314, Figure 4I). Consequently, we constructed the $dORP9^{MU}$-Flag vector (mutated the amino acids of the FFAT motif into Ala) and co-expressed with HA-VAP33 in S2 cells; no longer interaction was detected (Figure 4J; figure S5G), confirming VAP33 as an ER-anchor to reinforce ER-PM MCS structures.

To explore the role of Xkr-dORP9-VAP33 complex in maintaining ER-PM MCSs, we knocked down *tm9sf4*, *sac1*, *dorp9* and *vap33* in mCherry-Xkr and GFP-MAPPER expressing S2 cells, respectively, and we found *dorp9* and *vap33* disrupted the ER-PM MCSs structure, which resulted in less colocalization of Xkr and ER-PM MCSs (Figure S6), while cytoplasmic Xkr was still located at the ER-PM MCSs with a low expression of *tm9sf4* and *sac1*. This finding indicated that depleting Xkr resulted in the destabilization of the protein complex at the ER-PM junction, and consequently, the disappearance of the ER-PM MCS and ultimately decreasing PS accumulation in the PM. Collectively, these results demonstrated that Xkr can directly interact with dORP9 at ER-PM MCS to facilitate non-vesicular PS transport during apoptosis.

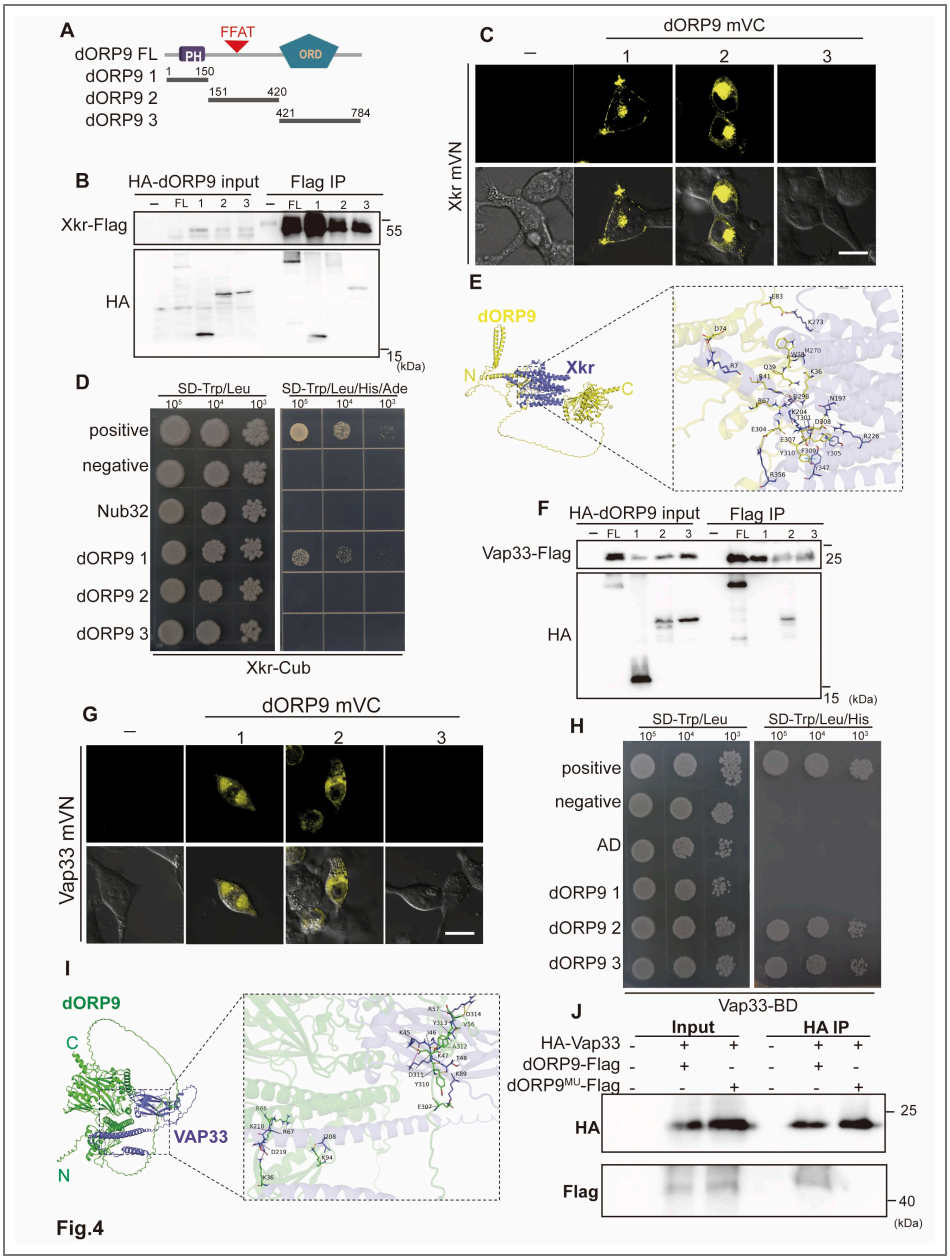

Figure 4. **OSBP-related protein OSBPL8 regulates apoptotic PS exposure via interacting with Xkr8**

Xkr cooperates with non-vesicular PS transport proteins to mediate efferocytosis *in vivo*

Given that Xkr interacted with dORP9 and VAP33 at ER-PM MCSs, TM9SF4 interacted with Sac1, we hypothesized that Xkr, TM9SF4, and dORP9 could exhibit a similar phagocytic phenotype in the same genetic pathway. In light of our above results showing that respectively suppressing *tm9sf4*, *sac1*, or *dorp9* in S2 cells led to an obvious reduction in efferocytosis, we next tested whether these proteins regulated efferocytosis *in vivo*. To this end, we characterized the efferocytosis phenotypes of $tm9sf4^{1}$, $sacl^{EY02269}$, and $dorp9^{S\text{-}532}$ mutants from the Bloomington *Drosophila* Stock Center. Relative expression analysis by RT-qPCR showed that all three mutants were likely null alleles (Figure S7A), and the numbers of macrophages and apoptotic cells in mutant embryos (at stage 13) did not significantly differ from those in WT embryos, suggesting that they do not regulate apoptosis or macrophage development in *Drosophila* (Figures S7B to S7G). The $tm9sf4^{1}$ and $dorp9^{s\text{-}532}$ embryonic macrophages both engulfed fewer apoptotic cells than macrophages in WT embryos, with a higher proportion of unengulfed than engulfed apoptotic cells, indicating impaired recognition and clearance of apoptotic cells (Figures 5A to 5H). However, the *sac1* mutant only exhibited slightly lower capacity for efferocytosis, with PIs of 2.05 ± 0.59. As *tm9sf4* RNAi displayed an efferocytosis phenotype more similar to that of xkr^{ko} *in vitro*, we speculated that *Sac1* deficiency could decrease the efficiency of PS translocation from ER to PM without completely abolishing it.

As our data showed that Xkr could physically interact with TM9Sf4 and dORP9, we next tested whether Xkr also genetically interacted with TM9SF4 and dORP9 in mediating cell corpse clearance by combining these mutations *in vivo*. To this end, we crossed xkr^{ko} mutant flies with $tm9sf4^{1}$ and $dorp9^{S\text{-}532}$ flies to obtain respective heterozygous double mutants. Efferocytosis assays in double mutant embryos indicated that $xkr^{ko}/tm9sf4^{1}$ and $xkr^{ko}/dorp9^{S\text{-}532}$ heterozygotes exhibited similarly impaired efferocytosis compared to WT flies, as that observed in homozygous single mutants (Figures 5D and 5G). Alternatively, macrophages in $xkr^{ko}/tm9sf4^{1}$ and $xkr^{ko}/dorp9^{S\text{-}532}$ heterozygous embryos failed to engulf more apoptotic cells (Figure 5F). Together, these results provide evidence of genetic interactions among *xkr*, *tm9sf4*, and *dorp9* in the efferocytosis of embryonic macrophages.

Human ORPs Xkr8 is required for the apoptotic PS exposure

In mammalian cells, Xkr8 undergoes C-terminal cleavage by caspase 3, leading to the release of activated Xkr8 fragments, which subsequently form heterotetramers with either basigin (BSG) or neuroplastin (NPTN). These heterotetramers then promote phospholipid scrambling during apoptosis [25]. And in some unidentified processes, Xkr8 can constitutively expose PS without an apoptosis stimulus in a phosphorylationdependent manner [42]. To assess whether PS transport from the ER to PM influences apoptotic PS exposure in mammals, we suppressed ORP expression in human HEK 293T cells using *xkr8* silencing by RNAi as a positive control. Flow cytometry assays with FITC-annexin V staining in HEK 293T cells treated with staurosporine (STS) to induce apoptosis showed that *xkr8*, *tm9sf4*, or *osbpl8* silencing resulted in significantly decreased PS exposure (Figure 6A, figure S8A). These results suggest that non-vesicular PS transport from the ER to the PM may also be required to regulate apoptotic PS exposure in mammals. Therefore, we investigated whether PS exposure mediated by non-vesicular PS transport was required for efferocytosis *in vitro*. For this experiment, we induced apoptosis in Jurkat cells with shRNA knockdown of *xkr8*, *htm9sf4*, *sacm1l*, *osbpl5*, and *osbpl8* encoded on a constitutive GFP expression vector, and then incubated these reporter mutants with RAW264.7 macrophages [43]. Quantification of phagocytic engulfment of each Jurkat knockdown cell line indicated that *xkr8* and *htm9sf4* knockdown resulted in reduced efferocytosis compared to that in untargeted RNAi control cells; *osbpl8* knockdown resulted in slightly reduced efferocytosis (Figures 6B and 6C, figure S8B).

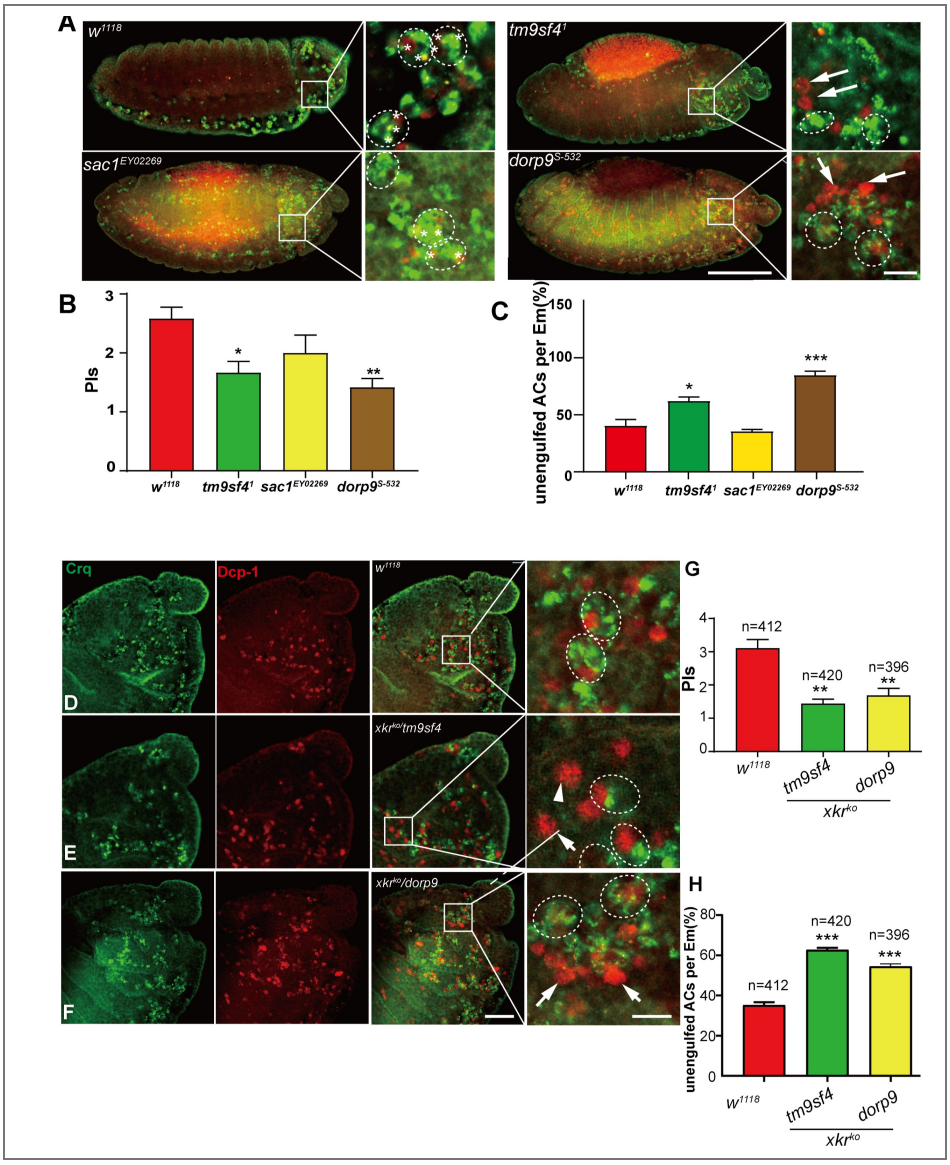

Figure 5. **Xkr regulates the non-vesicle transport of PS from ER to PM together with dORP9.**

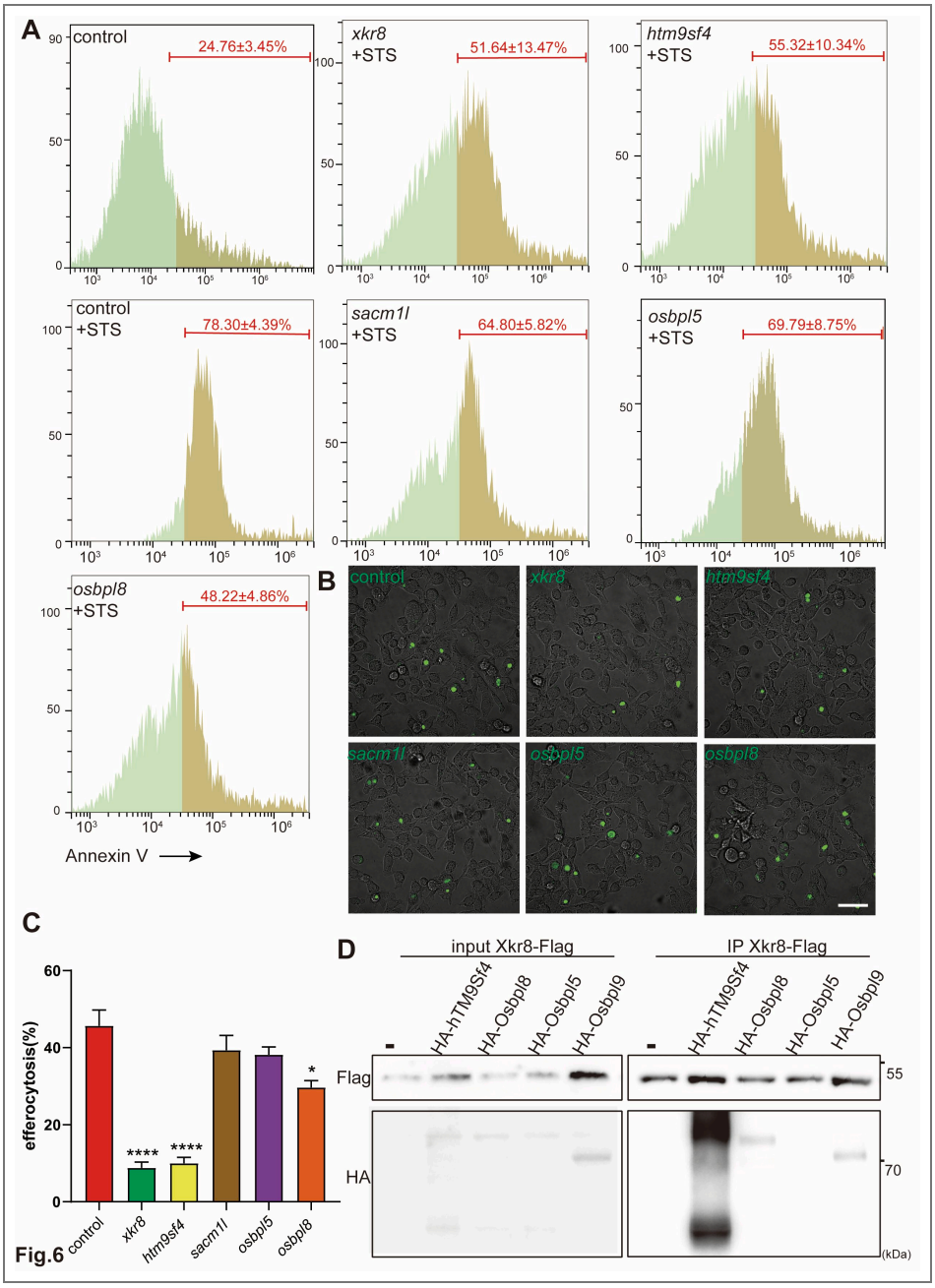

Figure 6. **Xkr interacts with transmembrane proteins TM9SF4 to regulate PS distribution**

As OSBP5/8 has been found to play important roles in non-vesicular PS transport via ER-PM MCS [38], and our above experiments showed that dORP9 could interact with Xkr in *Drosophila*, we sought to determine whether Xkr8 functions in conjunction with these ORP proteins to facilitate PS translocation from the ER to PM during apoptosis in mammalian cells. Co-IP assays in HeLa cells revealed that Xkr8 could interact with human OSBPL8 or OSBPL9, as well as human TM9SF4 (Figure 6D). This finding confirmed that transport of PS via ER-PM contact sites leads to efficient PS exposure and that interactions between Xkr8 and ORP5/8 regulate the entire process, ensuring PS is exposed in response to apoptotic signals.

Discussion

Our findings discover that the Xkr8 homolog in *Drosophila melanogaster*, Xkr, regulates non-vesicular transport of PS from the ER to the PM through direct interaction with the *Drosophila* ORPs (dORP9) to ensure efficient PS exposure upon apoptosis induction, triggering cell corpse recognition and clearance. Here, we show that Xkr protein level is increased in response to apoptotic signaling stimulation in a caspaseindependent manner, and the enhanced Xkr is enriched at ER-PM MCSs. The increased ER-PM MCSs may lead to the reinforced interaction between Xkr and dORP9, which in turn promotes the non-vesicular transport of PS from the ER to the PM through ER-PM contact sites, ultimately leading to PS externalization and efficient clearance of apoptotic cells. This mechanism is conserved from *Drosophila* to human macropahge (Figure 7).

As a classic and essential phospholipid scramblase, it has been clearly elucidated that *Caenorhabditis elegans* CED-8 and mammalian Xkr8 mediate apoptotic PS exposure in a caspase-dependent manner, respectively. Cleavage of an N-terminal EQED site of CED-8 or a C-terminal DXLD caspase recognition site of Xkr8 is required for their scramblase activation and the subsequent apoptotic cell clearance [44, 45]. The caspase activation is essential for the apoptotic PS exposure, whereas Xkr8 homolog in *Drosophila,* Xkr, lacks caspase recognition sites according to sequence alignment, and in native S2 cells, both C- and N-terminal eGFP-tagged Xkr showed a similar localization, mainly in the PM, partially in the cytoplasm, suggesting that Xkr activation may not require cleavage. Our study demonstrates that Xkr functions as a scramblase in the exposure of PS during apoptosis, a process essential for efficient efferocytosis both *in vivo* and *in vitro*. Previous studies have shown that in *Drosophila,* degenerated or damaged neurons expose PS to cause recognition and phagocytosis of dendrites by epidermal cells [46]. Overexpression of Xkr leads to ectopic PS exposure and a reduction of dendrites, suggesting that Xkr is involved in the PS exposure of damaged dendrites; but this PS exposure-mediated phagocytic process is independent of caspase activity, though it depends on the phagocytic receptor Draper on epidermal cells [23]. In addition, mouse Xkr8 activity in inducing apoptotic PS exposure has been reported to be stimulated by kinase-mediated phosphorylation, independent of caspase-mediated cleavage, suggesting that Xkr scramblase activity may also be regulated through an unidentified mechanism. Consistent with their finding, we found that apoptosis signal-induced increase in Xkr levels was regulated post-transcriptionally without caspase cleavage. Further research is required to investigate how apoptosis signals regulate Xkr amounts at the post-transcriptional level.

Based on these findings, we performed IP-MS analysis to identify proteins interacting with Xkr in regulating apoptotic PS exposure, and TM9SF4 was identified as a direct interaction partner of Xkr by Co-IP, Y2H, and BiFC assays. In human immune cells, TM9SF4 has been shown to increase phagocytic activity in metastatic tumor cells [47]. In *Drosophila*, *tm9sf4* mutant macrophages and *tm9sf4* knockdown S2 cells show a striking defect in phagocytosis of *Escherichia coli*-derived particles [34]. However, whether and how TM9SF4 is involved in apoptosis remains unclear. Our results showed that Xkr and TM9SF4 generally colocalize in the PM and, to a lesser extent, in the cytoplasm. Knockdown of *tm9sf4* in S2 cells disrupted the subcellular distribution of PS, inhibiting its exposure during apoptosis and subsequently impairing efferocytosis, whereas direct binding between TM9SF4 and Xkr promoted apoptotic PS exposure *in vitro* and *in vivo*. These data clearly demonstrate that TM9SF4 can regulate PS exposure, thus providing a previously undocumented caspase-independent mechanism of apoptotic PS exposure in efferocytosis.

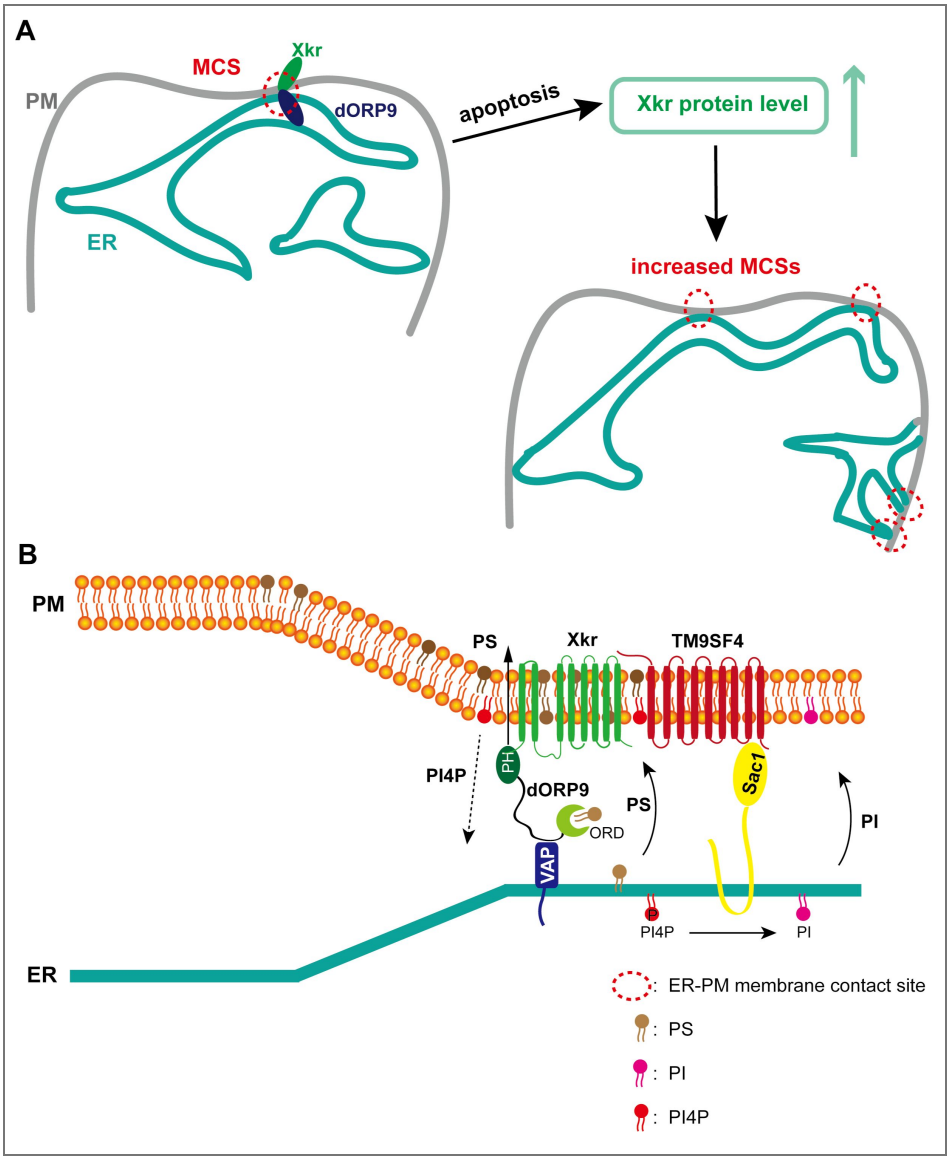

Figure 7. **Xkr regulates apoptotic PS exposure in *Drosophila*.**

As TM9SF4 has not been reported to participate in phospholipid transport, previous studies have shown that TM9SF4 can interact with the phospholipid phosphatase, Sac1, in human cells [35], which is consistent with our results that also identified TM9SF4 as a direct Sac1 interaction partner, whereas Sac1 does not directly interact with Xkr. Sac1, which primarily converts PI4P into phosphoinositides (PIs) at the MCS, plays a crucial role in establishing lipid gradients required for ORPs-mediated non-vesicular lipid transport [16]. We found that knockdown of *xkr*, *tm9sf4*, or *sac1* resulted in significantly increased PS localization to intracellular membrane structures (i.e., the ER and vacuoles) and reduced PS localization at the PM, whereas apoptosis signals could not restore the disorder PS localization. Furthermore, RNAi silencing of *tm9sf4* or *sac1* inhibited apoptotic PS exposure and phagocyte recognition. These cumulative results suggest that Xkr and TM9SF4 may regulate apoptotic PS exposure via non-vesicular PS transport at ER-PM contact sites. Our preliminary Sac1 knockdown data hint at a possible role for phosphoinositide regulation, but further studies are required.

Non-vesicular lipid transfer between membranes of different organelles is crucial for maintaining membrane homeostasis [48], with ORPs regulating intermembrane lipid transport in eukaryotes [15]. Non-vesicular PS transport was first reported in the homologous Osh/ORP proteins, Osh6 and Osh7, which localize to ER-PM contact sites in yeast. However, unlike vesicular transport, these proteins remain the only known lipid transporters with a demonstrated preference for PS substrate [49, 50]. In contrast, their mammalian orthologs, ORP5 and ORP8 [37, 50], are recruited to PM-ER contact sites to mediate PS-PI4P exchange between the PM and ER [51, 52]. Interestingly, our RNAi screen of OSBP homologs in *Drosophila* showed that knockdown of an OSBPL2 homolog, *CG3860* (dORP2), and an OSBPL9 homolog, *CG1513* (dORP9), but not ORP5/ORP8 homologs, resulted in obvious defects in PS exposure and efferocytosis in S2 cells, implying a role in non-vesicular PS transport.

We found that Xkr directly interacts with dORP9. Previous studies have shown that ORP9, along with the ORP5/8 ortholog ORP10/11, localizes to ER-trans Golgi network (TGN) contact sites and influences PS levels in the TGN[53]. Two recent studies found that these proteins could mediate PS-PI4P exchange between the ER and endocytic compartments for downstream processes such as recycling endosome fission [54] or lysosomal repair [55]. These findings support the possibility that ORP9 participates in lipid exchange at ER-endosome contact sites, while our results show that dORP9 regulates PS exposure during apoptosis via PS transport at ER-PM contact sites. dORP9 is expressed at ER-PM contact sites, and structural analysis revealed that dORP9 harbors both PH and ORD domains, which reportedly bind to PI4P in the PM and transport lipids, respectively [56]. As dORP9 lacks an ER TM domain, we hypothesized that other proteins might be required to stabilize its localization in the ER. We found that dORP9 directly interacts with VAP33 in the ER via its FFAT motif (EEDFYDAYDD), whereas Xkr directly interacts with its PH domain. However, Xkr showed no direct interaction with VAP33, suggesting dORP9 might serve as a bridge to connect VAP33 with Xkr, further reinforcing PM-ER contact sites to mediate PS transport. This similar mechanism was also observed in mice. In mouse WR19L T cells, another member of the Xkr family, Xk, participates in the exposure of PS mediated by ATP-P2X7 in a caspase-independent manner. Xk was found to interact with the lipid transporter protein VPS13A. VPS13A is primarily located at the contact sites between the ER and intracellular organelles, mediating phospholipid transport at the organelle membrane contact sites. Xk directly binds to the PH domain of VPS13A via its intracellular P—hairpin structure, enabling Xk to open the channel to scramblase P2X7-induced PS exposure. Defects in *Xk* and *vps13a* both lead to neuroacanthocytosis associated with McLeod syndrome, which may be caused by disrupted PS homeostasis [57]. However, the mechanism by which P2X7 activates the Xk-Vps13A complex to scramblase PS remains unclear, just as we are not clear about how the apoptosis signal activates the Xkr-dORP9 complex to expose apoptotic PS, although we proved that the interaction between Xkr and dORP9 is enhanced after apoptosis induction.

Taken together, this study reveals for the first time that apoptotic signaling induces post-translational upregulation of *Drosophila* Xkr, the assembly of the XKR-DORP9- VAP33 complex at the ER-PM contact site through direct binding to the PH domain of dORP9, and drives the non-

vesicular trafficking of PS from the ER to the PM. At the same time, Xkr cooperated with TM9SF4 module to achieve PS eversion and efficient phagocytosis of apoptotic cells. However, how apoptosis signals specifically "sense" and post-translationally regulate Xkr protein levels needs to be further illustrated. Meanwhile, as Xkr8 forms heterodimers with either Basigin (BSG) or Neuroplastin (NPTN), further studies are necessary to determine whether these molecules also participate in non-vesicular PS transport. Finally, we demonstrated that this PS transport mechanism, in which Xkr8/Xkr functions as a scramblase to expose PS while also mediating PS transfer from the ER to the PM is conserved between flies and mammals, which holds major implications for developing targeted therapeutics in several human diseases associated with defects in apoptosis and efferocytosis.

Materials and methods

Cell culture and transfection

Drosophila melanogaster Schneider's S2 cells were cultured in Sf-900TM II SFM (Gibco #10902088) containing 1% penicillin/streptomycin. Cells were incubated at 25 °C and transfected at 60-75% density with a DDAB suspension (250 μg/ml) [58].

Human embryonic kidney cell line HEK 293T and RAW 264.7 mouse macrophages were cultured in DMEM (Gibco) containing 10% FBS and 1% penicillin/streptomycin, and Jurkat cells were cultured in RPMI-1640 (Gibco) containing 10%FBS and 1% penicillin/streptomycin. Mammalian cells were incubated at 37°C and 5% CO2. Cell transfection was performed using Lipofectamine™ LTX and Plus Reagent (Invitrogen# 15338100), according to the manufacturer's instructions.

Double-stranded RNA production and RNAi treatment

Primers for generating specific double-stranded RNA (dsRNA) were obtained from the *D. melanogaster* RNAi Screening Center (DRSC), DRSC/TRiP Functional Genomics Resources (*harvard.edu*), and the T7 RNA polymerase sequence was added to the 5' end of each primer. dsRNA was generated using 1 μg of PCR product, followed by the High Yield RNA Synthesis Kit (NEB #E2040S) dsRNA synthesis. dsRNA sequences are shown in Table S1. S2 cells were treated with 10μg/ml dsRNA and incubated for 48h to get high RNAi efficiency. Cells were harvested to extract RNA or proteins, and apoptotic cells were added to observe phagocytic phenotypes using a confocal microscope (C2, Nikon Instruments).

Total RNA preparation and Quantitative Real-time PCR

Total RNA was extracted from S2 cells and flies using TRIzol reagent (Invitrogen, #15596026) and the Direct-zol RNA miniprep kit (Zymo Research, #R2052). RNA was reverse transcribed using the HiScript II 1st Strand cDNA Synthesis Kit (Vazyme #R211-02), and qPCR was performed using ChamQ Universal SYBR qPCR Master Mix (Vazyme #Q711-02) in an ABI Step One Plus instrument. Data represent the ratio or relative ratio of target mRNA levels to those of an internal reference gene (Rpl32). All experiments were performed in triplicate, with mRNA samples extracted from at least three biological replicates. The relative gene expression was quantified using the comparative method (ΔΔCT). The qPCR primers used for real-time quantitative PCR are listed in Table S2.

DNA Constructs

pAC-mCherry-Lact::C2 was used to indicate PS distribution. The pAC-mCherry-Lact::C2 were constructed first by PCR amplifying the bovine C2 domain (245-380aa) of mouse Lactadherin[59] and subsequently cloned into the pAC-mCherry vectors, using the XhoI and XbaI sites.

pAC-GFP-MAPPER or pAC-mCherry-MAPPER was used to indicate the ER-PM MCS. The MAPPER sequence was cloned as described by previous research [41]. Briefly, MAPPER contains: 1) a signal peptide (1-22aa) of human STIM1 in the N-terminal; 2) GFP or mCherry followed by STIM1 transmembrane (TM) domain (195- 240aa) with a downstream (GA)*6 linker sequence [60]; 3) FKBP12-rapamycin-binding (FRB) with a downstream (SAGG)*3 linker sequence; 4) the polybasic

tail (PB, 199-219aa) from human Rit tail [61]. To generate MAPPER, two helical linkers, (EAAAR)*4 and (EAAAR)*6, were cloned into the upstream and downstream flanking regions of the FRB, respectively.

Efferocytosis assay *in vitro*

Efferocytosis assays were performed as described previously [62]. Briefly, S2 cells were incubated with 5 μM CellTracker™ Red CMTPX (ThermoFisher#C34552) at 25°C for 1 h and then treated with 0.25 μg/mL Actinomycin D (AcD, MCE#HY-17559) at 25°C for 1 h, which has been demonstrated to induce apoptosis in S2 cells and exposure of PS on the surface of the dying cells[63]. Cells were collected by centrifugation at 1000 × g for 3 min and suspended in Sf-900TM II SFM. CMTPX-labeled prey cells (3×10^5 cells) were incubated with 1×10^5 S2 cells at 25°C for 60 min, and analyzed by confocal microscopy on glass-bottom 96-well plates (Thermo Fisher).

NBD-labeled phospholipid incorporation

Cells were stimulated with apoptotic stimuli, as described above. Centrifuge (1000×g, 3 min, room temperature) and wash the cells with 1 ml HBSS. The cells were centrifuged and washed with 1 ml HBSS/$CaCl_2$ (containing 1 mM $CaCl_2$), and then resuspended in 1 ml of cold HBSS/$CaCl_2$. Transfer 600 ml of the cell suspension to a 1.5-ml tube. Incubate the mixture in an aluminum block on ice for 7 min. Next, 600 ml of 200 nM NBD-PC (Avanti # 810130) in HBSS/$CaCl_2$ to the cell suspension (NBD-PC final concentration, 100 nM). Take 150 μl aliquots at 1, 2, 4, 6 and 8 min, mixed with 150 μl of lipid extraction buffer (HBSS/$CaCl_2$, 5 mg/ml fatty acid-free Bovine Serum Albumin) containing 500 nM Sytox Blue (Invitrogen, # S34857), and kept on ice. The Sytox Blue-negative population was analyzed for the incorporation of fluorescent lipids by flow cytometry.

Generation of *xkr*^{ko} S2 mutant cells

xkr sgRNA sequences were selected with an NGG PAM sequence in the genome. Two oligonucleotides for each target-Xkr sgRNA 1F: GATTTGCATCAACTGGAGCC; Xkr sgRNA 2R: GGCTCC AGTTGATGCAAATC were synthesized and annealed as previously described [64], ligations were performed with approximately 50 ng pAc-sgRNA-Cas9 vector and 2 ml annealed diluted ligonucleotides with T4 DNA ligase (NEB) in a 10 ml reaction volume for 2 h at 18 °C, and transformed into chemically competent *E. coli* DH5a. Positive clones were selected by colony PCR and sequenced with U6F. pAc-xkr sgRNA-Cas9 vector was transfected into S2 cells and selected by 5mg/ml puromycin (Sigma), a single cell was screened by 96-well plates, followed by temperature gradient PCR to identify *xkr* knockout cells.

Fly strains and genetics

The following *D. melanogaster* strains were obtained from the Bloomington Drosophila Stock Center: *TM9SF4*^{1}(BDSC#26653), *Sac1*^{EY02269}(BDSC#19651), *CG1513*^{MB07184}(BDSC#25259), *CG3860*$^{CR00915\text{-}TG4.1}$ (BDSC#81155), *Hml-GAL4>2xEGFP*, Chr2(BDSC#30140), *Hml-GAL4>2xEGFP*, Chr3(BDSC#30142), *vasa-cas9*(BDSC#51323), and *Crq-GAL4* (ffl) was a gift from Dr. Zongzhao Zhai (Hunan Normal University). The *pUAS-Xkr* were constructed in our laboratory. Briefly, selected genes were amplified by PCR and cloned into the Invitrogen pENTR/D-TOPO vector (Thermo Fisher # K242020). The Gateway™ LR Clonase™ II kit (Thermo Fisher #11791100) was used to transfer selected genes from the pENTR/D-TOPO vector to pPWG following the manufacturer's instructions. *xkr*^{ko} fly mutant was obtained by our lab. The *xkr* sgRNA constructs were constructed using *xkr* sgRNA oligos obtained from *http://targetfinder.flycrispr.neuro.brown.edu/*, as shown in Table S2. The constructs were verified by sequencing, and transgenic flies were generated by Unihuaii Inc. using the PhiC31 targeted integration system. The sgRNA transgenic flies were crossed with the *vasa cas9* strain to generate the Cas9-editing mutants, a single fly mutant was verified by qPCR and sequencing.

Antibody generation

The Xkr antibodies were obtained by immunizing mice in our laboratory. We synthesized two polypeptides of Xkr (from GL Biochem), 5-20AA and 194-206AA, respectively, and then mixed them with Freund's complete adjuvant, getting the antigen. Antibodies were raised by immunizing mice (*BALB/c*, 6-8 weeks old).

Protein extraction and western blotting

Protein samples were extracted and homogenized on ice in lysis buffer (50 mM Tris-HCl [pH 7.4], 1% TritonX-100, 0.15 M NaCl, 1 mM EDTA) with protease inhibitors. Lysates were centrifuged at 20000 x*g* for 30 min, and the supernatants were collected and quantified using the bicinchoninic acid assay. Equal amounts of protein were separated by SDS-PAGE on a 10-15% gradient gel, and transferred to a PVDF membrane (Millipore), which was blocked with fresh milk (5% in TBST) and incubated overnight with primary antibodies.

The antibodies were used at the following dilutions: mouse anti-actin (CST), 1:1000; mouse anti-Flag (Sigma) 1:1000; mouse anti-HA (CST) 1:1000; rabbit anti-Dcp-1 (CST, Cleaved *Drosophila* Dcp-1 (Asp215)) 1:400; rabbit anti-V5 (Beyotime) 1:1000; mouse anti-Crq 1:500, rabbit anti-Crq 1:400; mouse anti-Xkr 1:400. Anti-rabbit or anti-mouse horseradish peroxidase (HRP)-coupled secondary antibodies (Jackson Immuno Research Laboratories) were used at a 1:10000 dilution; ECL detection was performed according to the manufacturer's protocol (Pierce). All western blotting assays needed for quantitative analysis were repeated three times.

Immunoprecipitation and LC-MS/MS protein preparation

Plasmids encoding the differently expressed tagged proteins were co-transfected into S2 cells or 293T cells as previously described, and immunoprecipitation was carried out at 4 °C. Briefly, transfected cells were lysed in 50 mM Tris-Cl [pH 7.4], 1% TritonX-100, 0.15 M NaCl, 1 mM EDTA with protease inhibitor, and centrifuged. The supernatants were incubated with anti-FLAG M2 magnetic beads (Sigma#M8823) or anti-HA magnetic beads (CST#11846) for 2 h at 4 °C, beads were washed three times with TBS (50 mM Tris, 150 mM NaCl), and boiled in 2xSDS loading buffer for 5 min. For Co-IP assays, the supernatants were analyzed by western blotting. For LC-MS/MS analysis, 5 μl of the supernatants were loaded onto an SDS-PAGE gel, followed by silver staining. The rest of the samples were sent to HOOGEN BIOTECH company (Shanghai, China) for LS-MS/MS analysis. The MS/MS analysis was performed using three independent biological repeated samples.

Yeast two-hybrid assays

For binary yeast two-hybrid assays, transmembrane proteins use the split-ubiquitin system, which inserts genes of interest into Cub or Nub as vectors and transforms vectors into yeast THY.AP4 [65]. Yeast competent cells were obtained using LiAc solution, as previously described, and transformed with target gene-Cub or Nub vectors. The mixture was stirred and incubated at 30 °C for 30 min, followed by heat shock treatment at 42 °C for 40 min. The yeast cells were then centrifuged at 2000 ×g for 1 min, washed with 100 μL of sterile water, resuspended in 50 μL of sterile water, plated on synthetic-defined (SD)-Leu/Trp dropout plates, and grown for 3-4 days at 30 °C. Finally, three representative colonies were selected and diluted for spot testing. The interaction was detected using SD-Ade/His/Trp/Leu plates.

Bimolecular fluorescence complementation (BiFC)

BiFC analysis enables the direct visualization of protein interactions in living cells. The two fluorescein fragments of mVenus were fused to two candidate interacting proteins, and the fragments formed a fluorescent complex when the two proteins interacted with each other [66]. The two proteins whose interactions were to be detected were cloned into pcDNA3.1-mVenusN and pcDNA3.1-mVenusC vectors, coding for the N-terminal (VN) and C-terminal (VC) fragments of

mVenus, respectively, and transfected into 293T cells using the PEI method. After 48 h of culture, the fluorescence complementarity results were observed by confocal laser microscopy. If the two proteins interact, they excite yellow fluorescence.

Embryo immunostaining

Immunostaining was performed as previously described [67, 68]. Briefly, *Drosophila* embryos at stage 13 were fixed in 4% paraformaldehyde and stained with relevant antibodies, i.e., Crq specifically labels macrophages while Dcp-1 labels ACs. The goat anti-rabbit Alexa Fluor Plus 594-coupled or anti-mouse Alexa Fluor Plus 488-coupled secondary antibodies (Jackson Immuno Research Laboratories) were used at a 1:1000 dilution. Stained embryos were mounted in Vecta Shield medium, observed using confocal laser microscopy (C2, Nikon Instruments), and photographed at 20* and 100* magnifications. Images were processed using the Adobe Illustrator software. The phagocytosis ratio was quantified as the number of engulfed ACs compared to the total ACs, and PI was quantified as previously described [68, 69]. The PI was calculated from confocal images taken from five embryos and three confocal image stacks per embryo.

Cell immunofluorescence assay

S2 cells were plated on a cover glass, fixed in 4% paraformaldehyde for 5 min, incubated in 1% bovine serum albumin (BSA) in 0.1% PBS-Tween for 1 h, and then incubated with the antibody overnight at 4 °C in PBS containing 1% BSA and 0.1% Tween. Alexa Fluor 488-conjugated goat anti-mouse antibody was used at a 1:500 dilution for 1 h. Hoechst 33342 was used to stain the cell nuclei. The samples were imaged using confocal laser microscopy (C2; Nikon Instruments).

Molecular modeling of Xkr, Vap33, and dORP9

The protein sequences of Xkr, Vap33, and dORP9 were downloaded from Flybase(*https://flybase.org/*), and the structures of the Xkr, Vap33, and dORP9 proteins were calculated using the AlphaFold3 server[70]. The output prediction model was rigorously evaluated for quality. Finally, the prediction results were visualized in three dimensions and analyzed in depth for the interaction interface using PyMol software (version 3.1.4). In brief, AlphaFold 3 generated five alternative models along with their corresponding confidence scores. We mainly relied on the interface template modeling score (ipTM > 0.6) to select the optimal model for subsequent analysis. The optimal complex structure model predicted by AlphaFold 3 was imported into the PyMOL molecular graphics system for visualization and interaction analysis. After the nonpolymer ligands were deleted and only the protein backbone was retained in PyMOL; we predicted the binding interface of protein A and protein B through hydrogen bond and salt bridge analysis, hydrophobic interaction analysis, and interface area calculation. Further ray-tracing rendering is used to generate high-resolution illustrations.

Apoptosis induction of Jurkat cells and efferocytosis assay by Raw264.7 cells

Jurkat human leukemia T cells treated with the broad-spectrum protein kinase inhibitor staurosporine (Sts) were used as a model for apoptosis, which causes activation of executioner caspases [71]. Briefly, Jurkat cells transfected with shRNA-pGreen vectors were treated with 10nM Sts at 37°C for 60 min. The cells were then collected by centrifugation at 500 g for 5 min and suspended in DMEM-10% FCS. Apoptotic Jurkat cells were added to Raw264.7 cells at a ratio of 10:1 and incubated at 37°C for 6h. After washing with PBS, the phagocytes were suspended in 100 μl of PBS containing 2% FCS and analyzed by confocal microscopy on 96-well glass-bottom plates (Thermo Fisher Scientific).

Phylogenetic tree

Firstly, collect homologous protein sequences through public databases (such as Flybase, NCBI) to make a fasta file, and then perform sequence alignment using Mega11 software. The phylogenetic tree was generated by the maximum likelihood method.

Statistical analysis

Statistical analyses were performed using the GraphPad Prism software. Data are presented as the mean ± SEM. One-way analysis of variance (ANOVA) or Student's *t*- test was used to determine statistical significance. "*" stands for $p < 0.05$, "**" for $p < 0.01$, "***" for $p < 0.001$, and "****" for $p < 0.0001$. For efferocytosis statistics in flies, at least five embryos from each genotype were tested, unless otherwise indicated.

Data availability

All data needed to evaluate the conclusions in the paper are present in the paper and/or the Supplementary Materials. The mass spectrometry proteomics data have been deposited to the ProteomeXchange Consortium via the PRIDE partner repository with the dataset identifier PXD058895.

Supplementary information

Table S1. dsRNA primers used in this paper

Gene	Forward	Reverse
xkr	CGCGTATGTGGCCAGTAT	TAAGTACGCACAGTATTTGGA
tm9sf4	GGAGAGACGCAGCTATATTT	TCGCGACCCTTCATTGTT
sac1	CGGGCACACGGCTCTT	CTGCGTGGACACCAATTTG
cg1513	GGGACAAGGAAAGCCTTTAG	CAGCATTCTCGTCCAGAAC
cg3860	CCGTATCAGCATTAGCCTC	GAAACTCGACGGTCACAG
cg9205	ATGGCAGTACCGTTGGTTT	TTGTTCCGTGAGAAACAGAG
cg42668	GCAGCAGCCCGCAAC	ACGCCCAGCGATTGGT
cg6708	GTAGTAGCGAGGACCAGG	CAGCAGCGGATTGAAGG
vap33	GACTAAACCGGGGACCGTAT	TGTGAGGGATTTCATAGGGC
dcp-1	GCGGTGGCCATACTCTC	GAACAGCTTCGGCTTGC

Add T7 promoter taatacgactcactatagggaga to each primer 5'end.TAATACGACTCACTATAGGGGGGA

Table S2. qPCR and sgRNA primers used in this paper

Gene	Forward	Reverse	Reference
Rpl32	CCTCTCAACGTATTGCAGAC	GTAAATGAACACTGCGAAGATTATG	This paper
xkr	GAATCAGCACCGCAGAAAATAC	AGGCGATTGGAGTGATTGTAC	This paper
cg1513	AAGGTCAAGTAATAGGCAAGGG	GTCGTAGGCATCGTAGAAGTC	This paper
tm9sf4	ACTTATTTCCAGCTCTGCGG	CGTCGGTATGAACTCTGTGATC	This paper
cg3860	GGTAACTTGGATGGTGCCTC	CTTTGTATGTGGGTTAGTTGCG	This paper
vap33	GCTGCGTGAATGCAACATTG	AAAGACCGGAATCTGCTTCTC	This paper
sac1	ATCCACAAGTGCGATACGAG	GATAGACACCGAACTGATCCTG	This paper
xkr8	GCAGCTGGGTTACCTGTAC	GTCTCGAAGAGCCGCAG	This paper
osbpl5	ACAGCCGCACATTCTACATAG	AGCGAGTTCCCATAAAACCTG	This paper
osbpl8	GAATCCAACACCTGACATTAAGC	TCTTGGGTAGCTTCAGTTTGG	This paper
sacm1l	GCGATGCTAAACCATGTCTTG	TCCATACAAACCGCTGATCTG	This paper
vapb	GATATGGAAGCAGTATGGAAGGAG	CTGTCTTTGATGCAGTTGTGG	This paper
htm9sf4	GGTGTTTGGCGGATTTTCTG	GAGTGCTTTCCCCAAATGAAG	This paper
xkr sgRNA1	ttcGCACATGTGCAATAAGGAGG	aacCCTCCTTATTGCACATGTGC	This paper
xkr sgRNA2	ttcGAAGTGGACGCCCTTATGAT	aacATCATAAGGGCGTCCACTTC	This paper
xkr sgRNA3	ttcGATTTGCATCAACTGGAGCC	aacGGCTCCAGTTGATGCAAATC	This paper

Table S3. Key resources

REAGENT or RESOURCE	SOURCE	IDENTIFIER
Antibodies		
Rabbit monoclonal anti-HA-Tag (C29F4)	Cell Signaling Technology	Cat#3724; *RRID:AB_1549585*
Rabbit monoclonal anti-V5-Tag	Beyotime	Cat #AZ050
Mouse monoclonal anti-FLAG® M2 Antibody	Sigma-Aldrich	Cat#F1804; *RRID:AB_262044*
Rabbit polyclonal anti-Cleaved Drosophila Dcp-1 (Asp215)	Cell Signaling Technology	Cat #9578
Rabbit polyclonal anti-Crq	This paper	N/A
mouse polyclonal anti-Xkr	This paper	N/A
Perxidase-conjugated AffiniPure Goat Anti-Rabbit IgG(H+L)	Jackson ImmunoResearch	Cat#111-035-003; *RRID:AB_2313567*
Perxidase-conjugated AffiniPure Goat Anti-Mouse IgG(H+L)	Jackson ImmunoResearch	Cat#115-035-003; *RRID:AB_10015289*
Bacterial and virus strains		
DH5α	TaKaRa	Cat#9057
BL21	TaKaRa	Cat#9126
BL21 (DE3)	Solarbio	Cat#C1400
Y2HGold	Clontech	Cat#630498
THY.AP4	This paper	N/A
Biological samples		
Chemicals, peptides, and recombinant proteins		
TRIzol Reagent	Invitrogen	Cat#15596026
CellTracker™ Red CMTPX	Thermofisher	Cat#C34552
Sytox Blue	Invitrogen	Cat# S34857
16:0-06:0 NBD PC: 1-palmitoyl-2-{6-[(7-nitro-2-1,3-benzoxadiazol-4-yl) amino] hexanoyl}-sn-glycero-3-phosphocholine	Avanti Research	Cat#810130
Puromycin	Sigma-Aldrich	Cat#540411

Critical commercial assays		
Annexin V apoptosis kit	Invitrogen	Cat#V13241
Hoechst 33342	Thermo Scientific	Cat#H3570
Pierce™ Anti-HA Magnetic Beads	Thermo Scientific	Cat#88837
Anti-FLAG® M2 magnetic beads	Sigma-Aldrich	Cat#M8823
HA-Tag (C29F4) Rabbit mAb (Magnetic Bead Conjugate)	Cell Signaling Technology	Cat#11846
HiScript® III RT SuperMix for qPCR (+ gDNA wiper)	Vazyme	Cat#R323
ChamQTM Universal SYBR® qPCR Master Mix	Vazyme	Cat#Q711
Experimental models: Cell lines		
Human: HEK293T cells	FuHeng Cell Center	Cat#FH0244
Human: Jurkat Clone E6-1 cells	YiZeFeng Biotechnology Co., LTD	Cat#YCL-0374
Mouse: RAW264.7 cells	YiZeFeng Biotechnology Co., LTD	Cat#YCL-0337
Human: HEK293TN cells	This paper	N/A
Drosophila: S2 cells	This paper	N/A
Drosophila: S2 cells (xkr^{ko})	This paper	N/A
Experimental models: Organisms/strains		
D. elanogaster: w^{1118} (WT)	This paper	N/A
D. elanogaster: BDSC#26653: $TM9SF4^{1}$	Bloomington Drosophila Stock Center	N/A
D. elanogaster: BDSC#19651: $Sac1^{EY02269}$	Bloomington Drosophila Stock Center	N/A
D. elanogaster: BDSC#25259: $CG1513^{MB07184}$	Bloomington Drosophila Stock Center	N/A
D. elanogaster: BDSC#81155: $CG3860^{CR00915\text{-}TG4.1}$	Bloomington Drosophila Stock Center	N/A
D. elanogaster: BDSC#30140: *Hml-GAL4>2xEGFP*, Chr2	Bloomington Drosophila Stock Center	N/A
D. elanogaster: BDSC#30142: *Hml-GAL4>2xEGFP*, Chr3	Bloomington Drosophila Stock Center	N/A
D. elanogaster: BDSC#51323: *vasa–cas9*	Bloomington Drosophila Stock Center	N/A
D. elanogaster: xkr^{ko}	This paper	N/A
Oligonucleotides		
all Oligonucleotides-Please see Table S1 and S2	This paper	N/A
Recombinant DNA		
pAC5.1-XKR-GFP	This paper	N/A
pAC5.1-GFP-XKR	This paper	N/A
pAC5.1-XKR-Flag	This paper	N/A
pAC5.1-XKR-mCherry	This paper	N/A
pAC5.1-XKR sgRNA-cas9	This paper	N/A
pAC5.1-mCherry-CG1513	This paper	N/A
pAC5.1-mCherry-CG3860	This paper	N/A
pAC5.1-mCherry-TM9SF4	This paper	N/A
pAC5.1-GFP-Sac1	This paper	N/A

pAC5.1-mCherry-Lact::C2	This paper	N/A
pAC5.1-GFP-Rab5	This paper	N/A
pAC5.1-GFP-Rab7	This paper	N/A
pAC5.1-GFP-KDEL	This paper	N/A
pAC5.1-GFP-LAMP	This paper	N/A
pAC5.1-GFP-GM130	This paper	N/A
pMD18T	This paper	N/A
PCR8	This paper	N/A
attB	This paper	N/A
pET28a-XKR	This paper	N/A
pNubWT	This paper	N/A
pNubXgate32-Tm9sf4	This paper	N/A
pBait-Cub-XKR	This paper	N/A
pNubXgate32-Sac1	This paper	N/A
pBait-Cub-Tm9sf4	This paper	N/A
pNubXgate32-CG1513 1-150	This paper	N/A
pNubXgate32-CG1513 151-420	This paper	N/A
pNubXgate32-CG1513 421-784	This paper	N/A
pNubXgate32-CG9205	This paper	N/A
pNubXgate32-CG1513	This paper	N/A
pNubXgate32-CG3860	This paper	N/A
pNubXgate32-Vap33	This paper	N/A
pAC5.1-mCherry-MAPPER	This paper	N/A
pAC5.1-GFP-MAPPER	This paper	N/A
pAC5.1-HA-TM9SF4	This paper	N/A
pAC5.1-HA-CG3860	This paper	N/A
pAC5.1-HA-CG1513	This paper	N/A
pAC5.1-HA-CG1513 1-150	This paper	N/A
pAC5.1-HA-CG1513 151-420	This paper	N/A
pAC5.1-HA-CG1513 421-784	This paper	N/A
pAC5.1-HA-Vap33	This paper	N/A
pAC5.1-HA-CG9205	This paper	N/A
pAC5.1-Sac1-Flag	This paper	N/A
pAC5.1-V5-Sac1	This paper	N/A
pCDNA3.1-XKR-mVenusN	This paper	N/A
pCDNA3.1 -CG3860-mVenusC	This paper	N/A
pCDNA3.1 -CG3860-mVenusN	This paper	N/A
pCDNA3.1-Vap33-mVenusN	This paper	N/A
pCDNA3.1 -CG1513-mVenusC	This paper	N/A
pCDNA3.1 -CG1513 1-150-mVenusC	This paper	N/A
pCDNA3.1 -CG1513 151-420-mVenusC	This paper	N/A
pCDNA3.1 -CG1513 421-784-mVenusC	This paper	N/A
pCDNA3.1 -TM9SF4-mVenusC	This paper	N/A
pCDNA3.1 -Sac1-mVenusN	This paper	N/A
pCDNA3.1-Xkr8-Flag	This paper	N/A
pCDNA3.1 -HA-hTM9SF4	This paper	N/A

pCDNA3.1 -HA-OSBPL5	This paper	N/A
pCDNA3.1 -HA-OSBPL8	This paper	N/A
pCDNA3.1 -HA-OSBPL9	This paper	N/A
pGreen xkr8	This paper	N/A
pGreen htm9sf4	This paper	N/A
pGreen sacml1	This paper	N/A
pGreen osbpl5	This paper	N/A
pGreen osbpl8	This paper	N/A
pGreen osbpl9	This paper	N/A
Software and algorithms		
SMART	EMBL	*https://smart.embl.de/*
ImageJ	NIH	*https://imagej.net/ij/download.html*
MEGA 12	MEGA	*https://www.megasoftware.net/*
GraphPad Prism 8	GraphPad Software	*https://graphpad-prism.software.informer.com/8.0/#google_vignette*
Pymol	DeLano Scientific LLC	*https://pymol.org/*
AlphaFold3	Google	*https://alphafoldserver.com/*
CytExpert	BECKMAN	*https://www.mybeckman.cn/flow-cytometry/research-flow-cytometers/cytoflex/software*
Other		

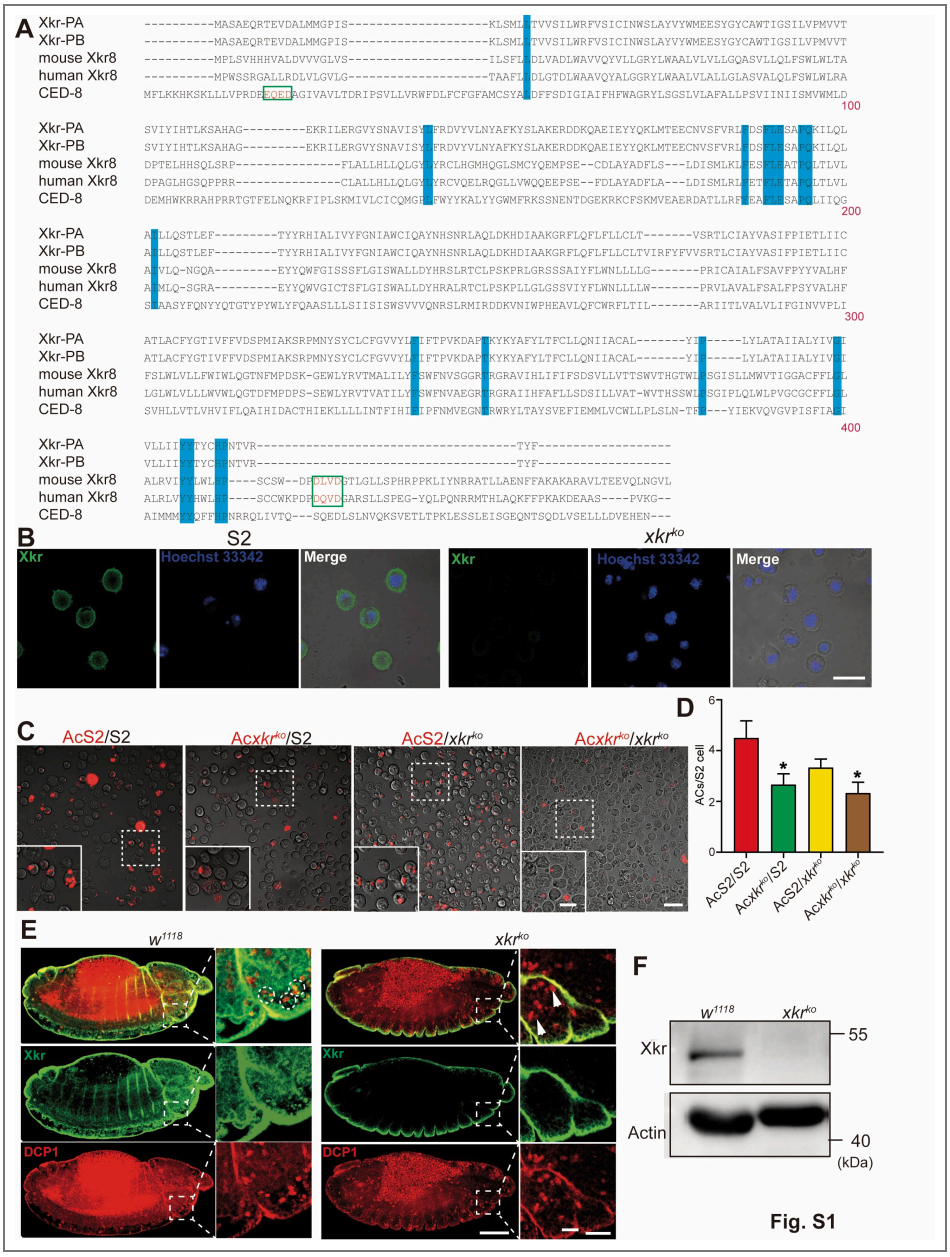

Fig. S1. *xkr*^{ko} results in efferocytosis defects by decreasing apoptotic PS exposure.

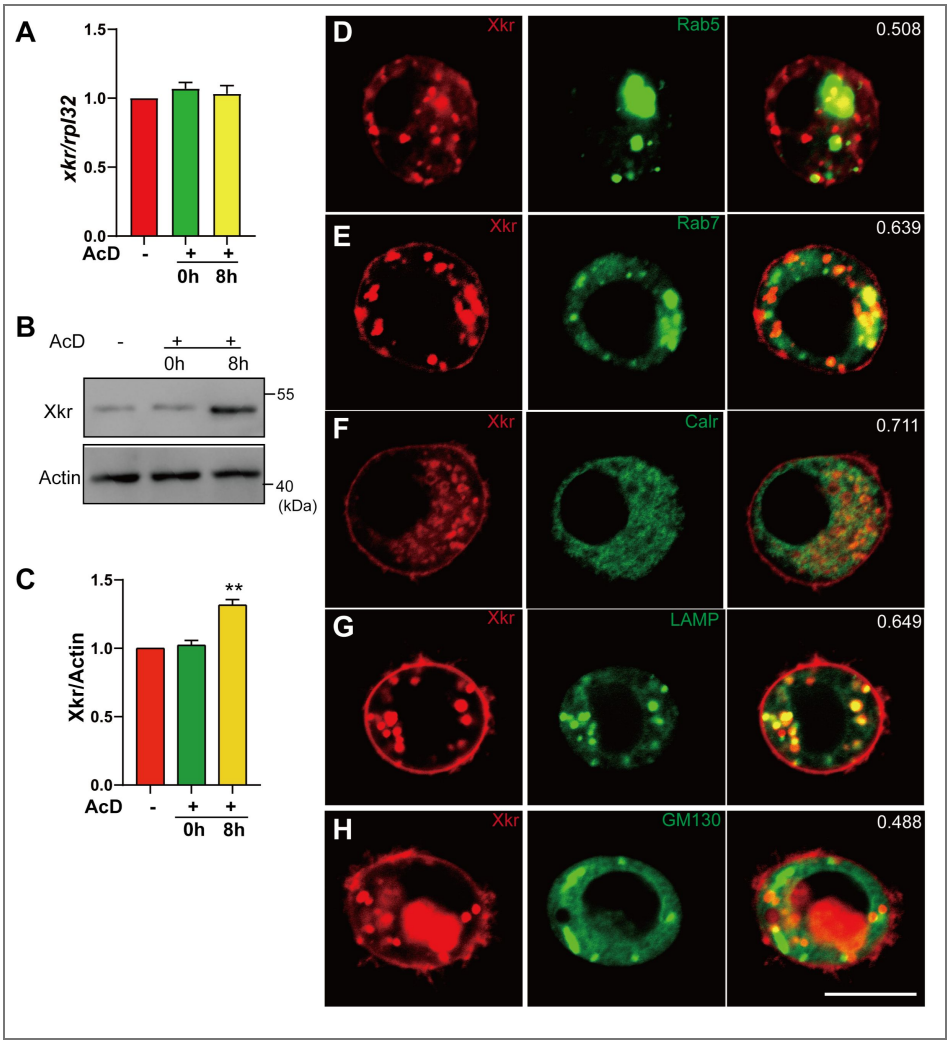

Fig. S2. The protein level of Xkr was induced by apoptosis and Xkr expressed in the internal membrane.

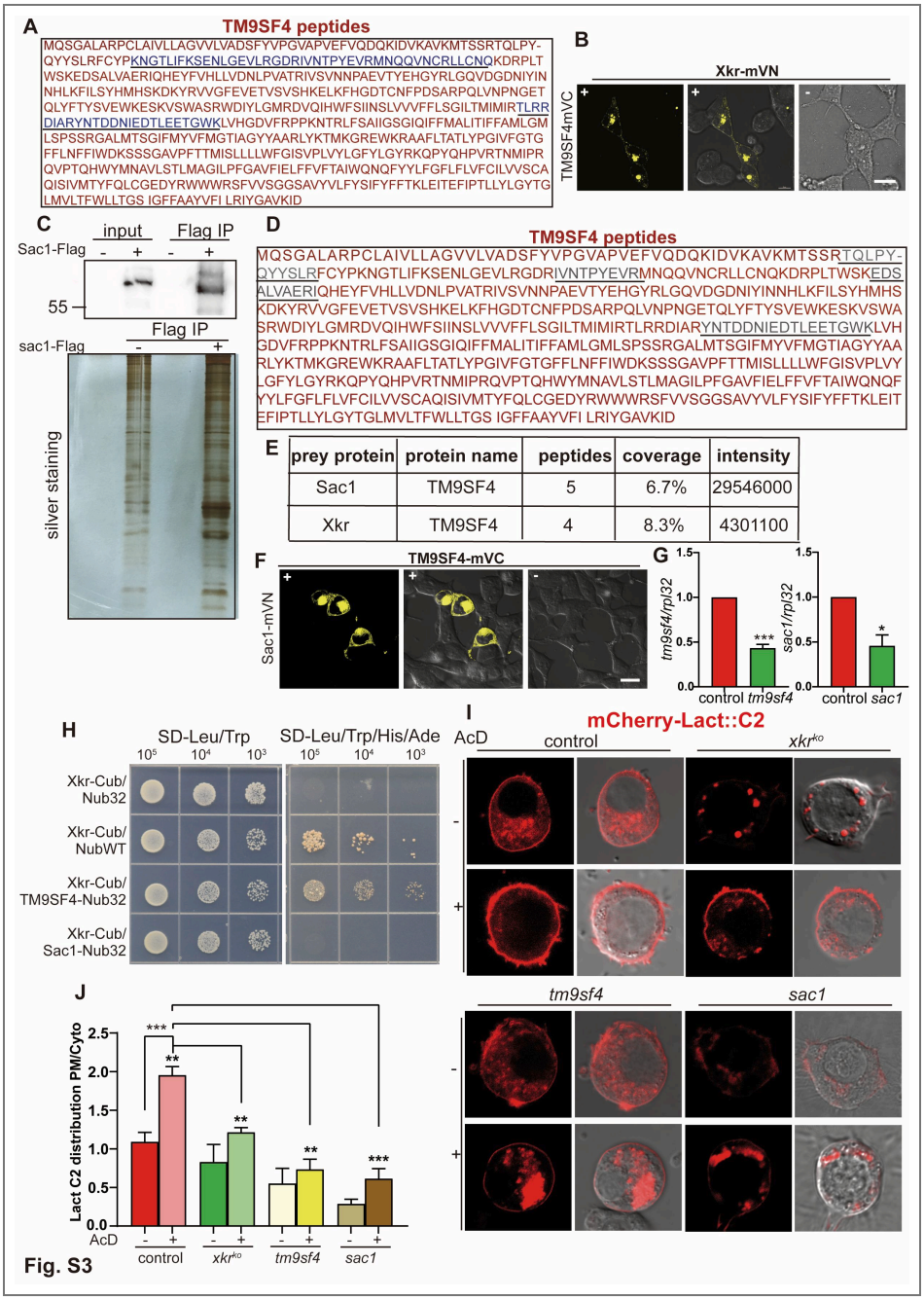

Fig. S3. Xkr, TM9SF4 and Sac1 regulate the PS distribution during apoptosis.

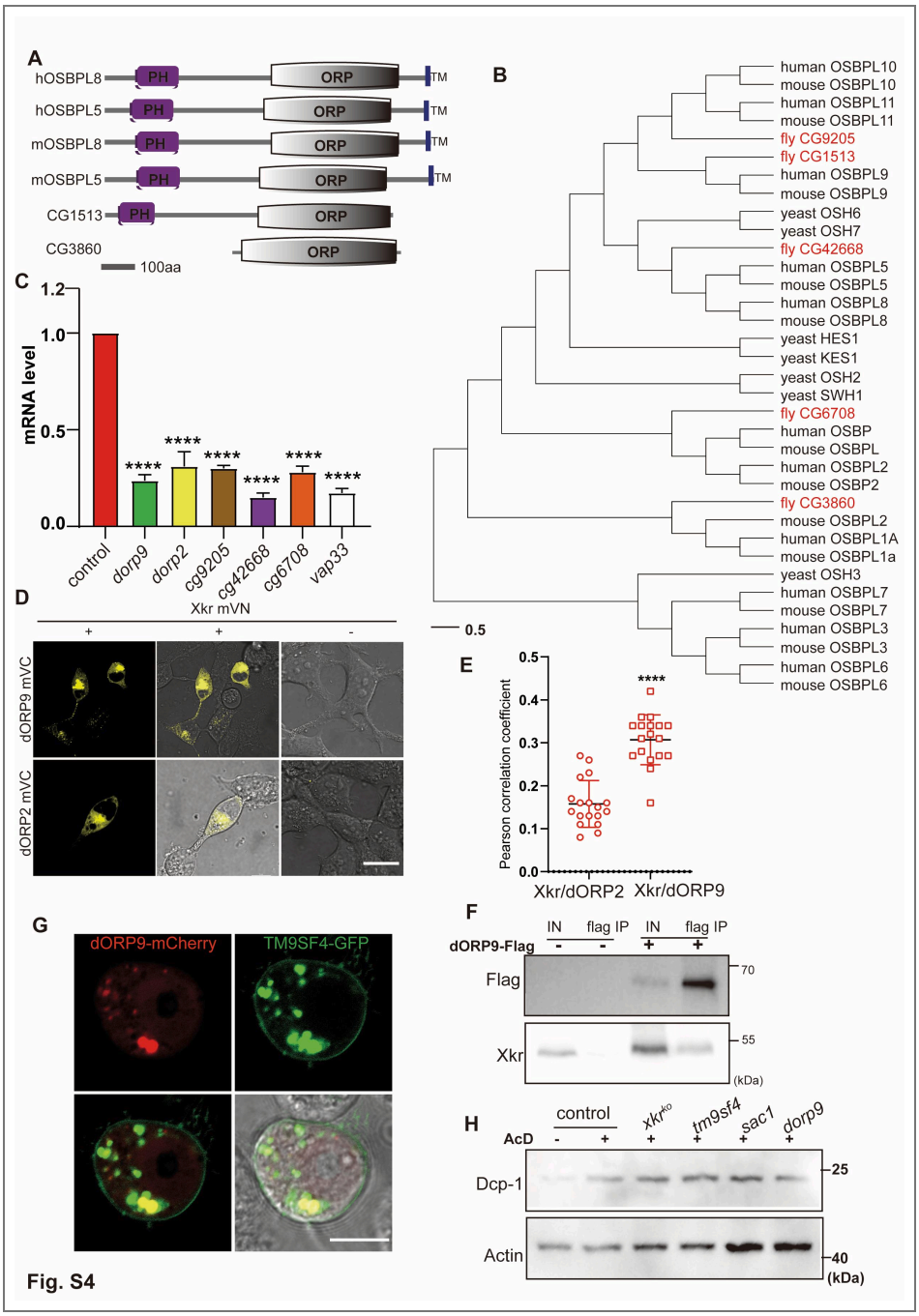

Fig. S4

Fig. S4. Xkr interacts with dORP9 and dORP2, and Xkr protein level is induced by apoptosis.

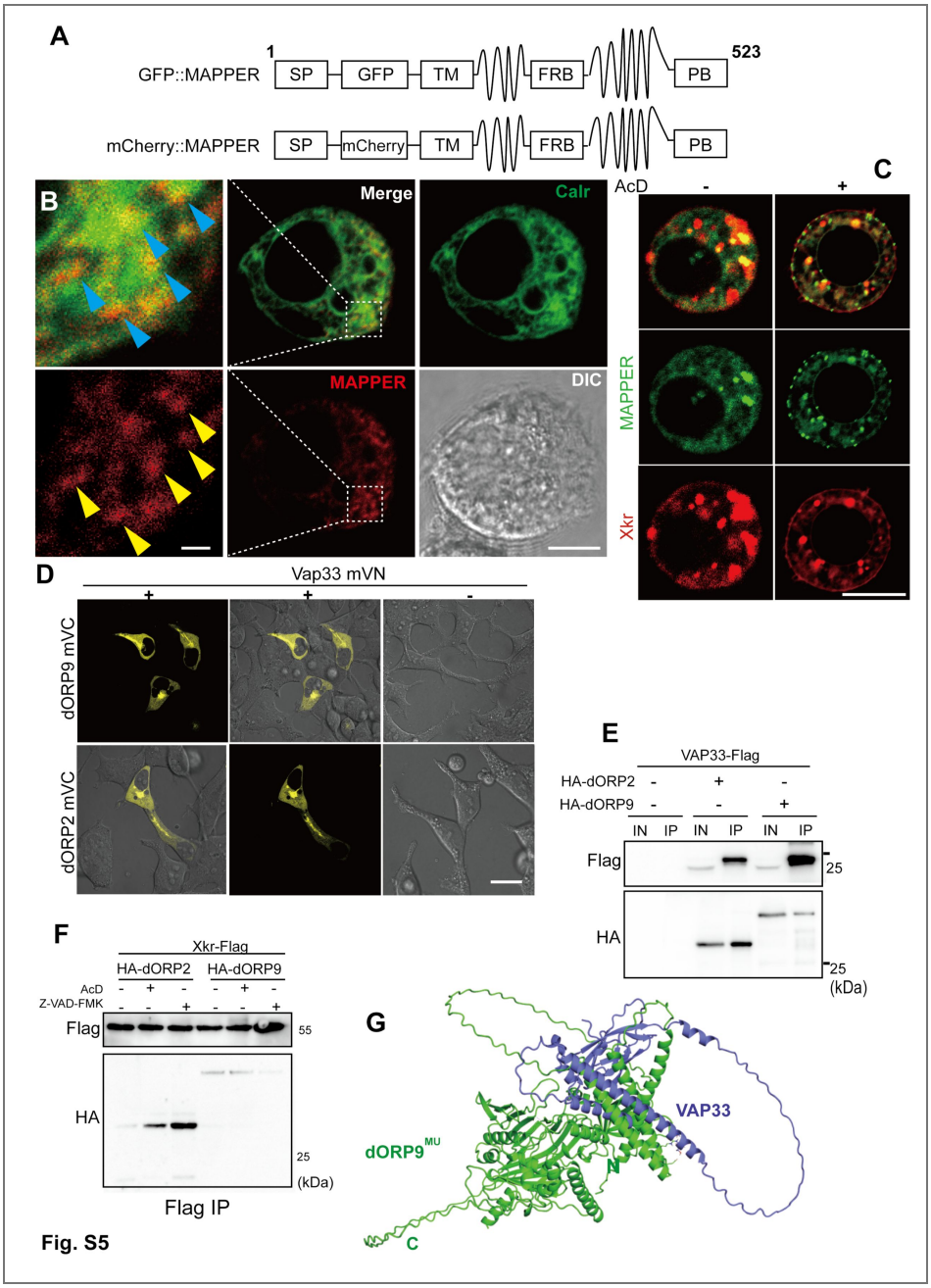

Fig. S5. dORP9 interacted with VAP33, and apoptosis elevated the interaction between dORP9 and Xkr in S2 cells.

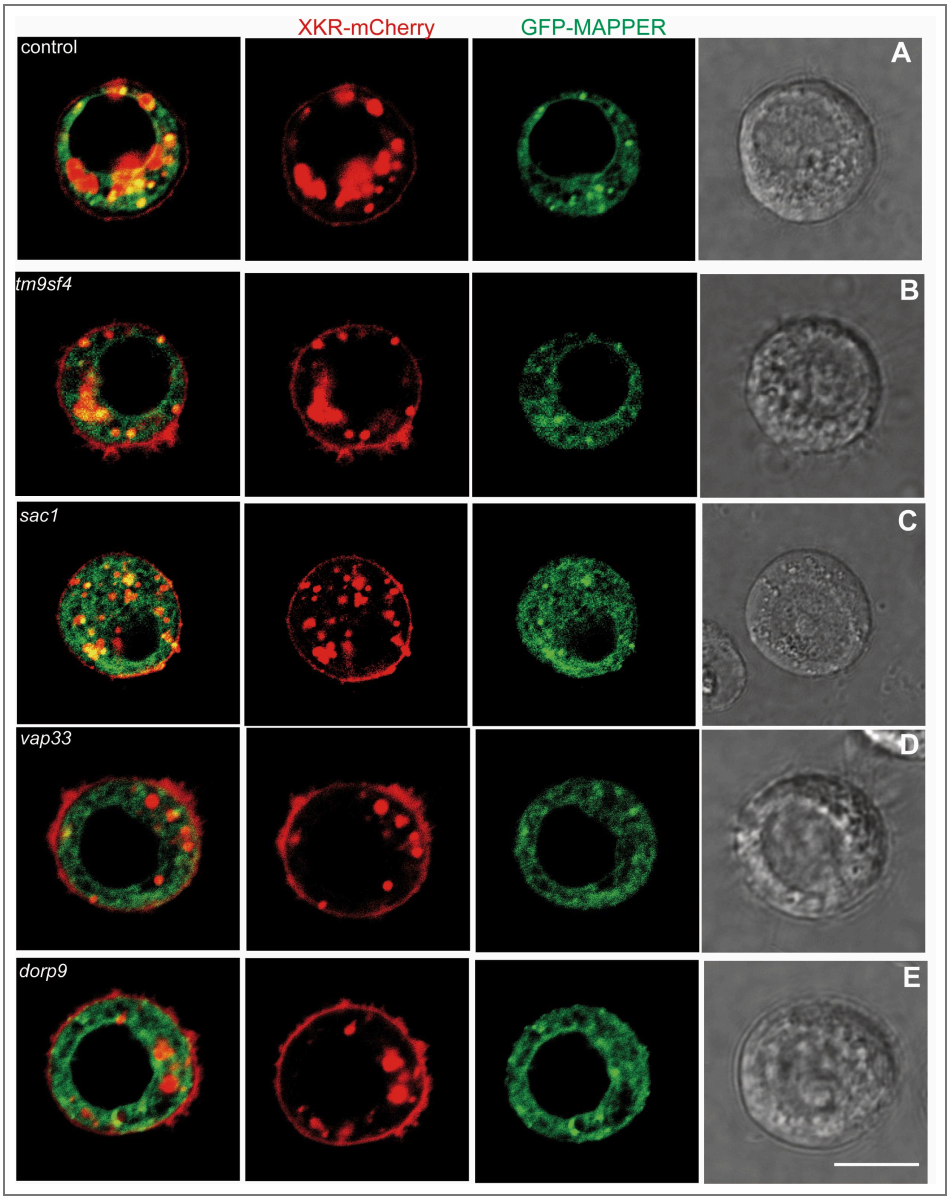

Fig. S6. **dORP9 and VAP33 disrupt the binding of Xkr to ER-PM MCSs.**

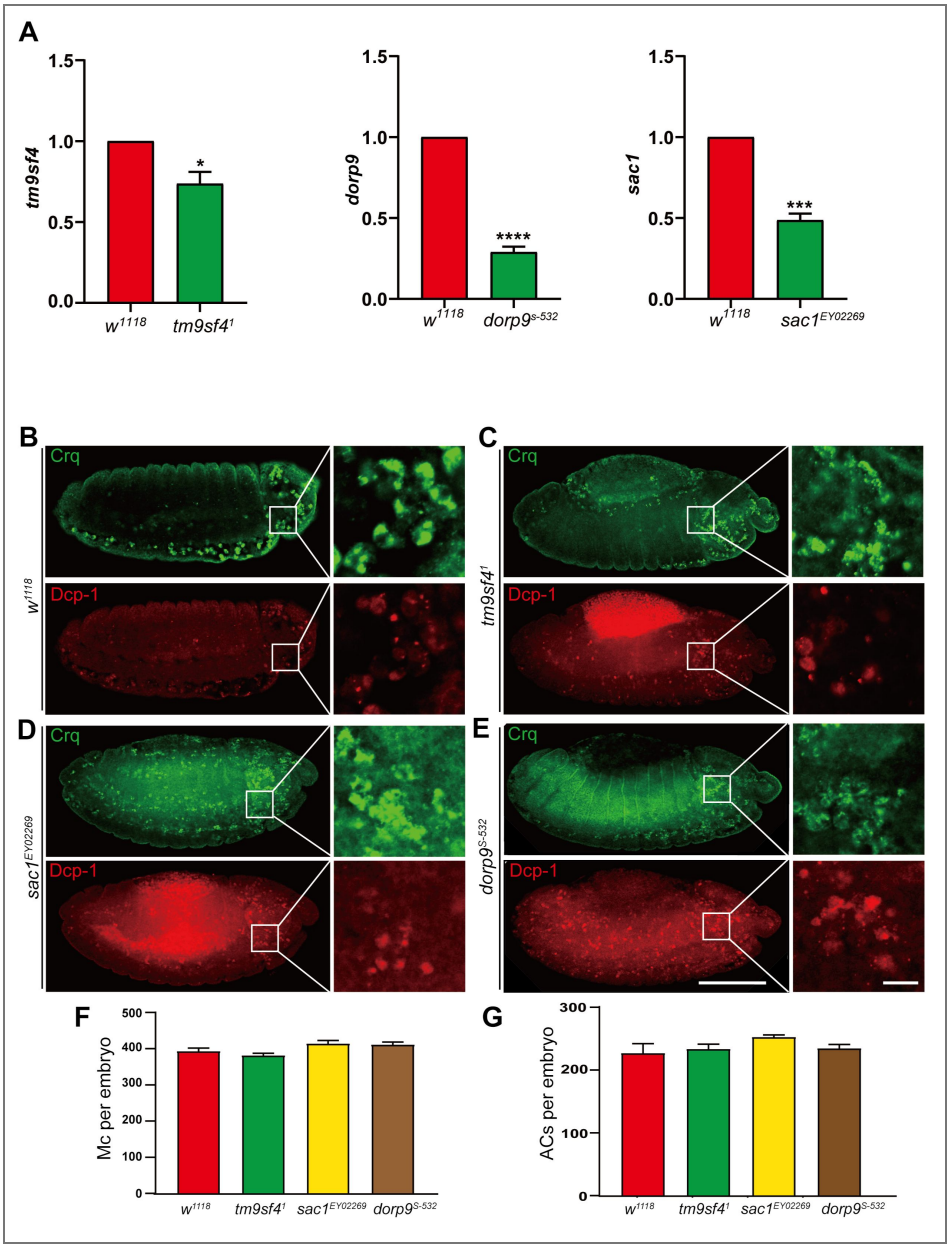

Fig. S7. ***tm4sf4*, *sac1* and *dorp9* do not affect macrophages or ACs development in fly embryos.**

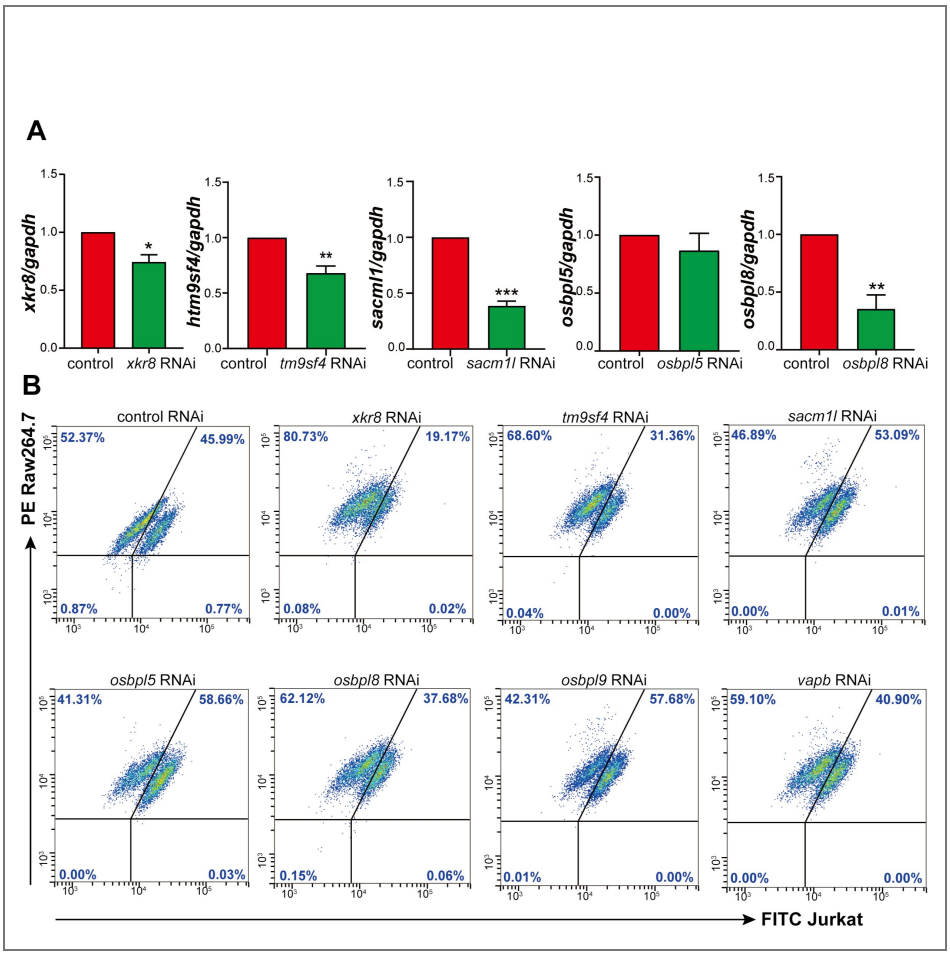

Fig. S8. The low expression of *xkr8*, *htm9sf4* and *sacm1l* in apoptotic Jurkat cells results in inefficient efferocytosis by macrophages.

Acknowledgements

We thank the Bloomington *Drosophila* Stock Center for the *Drosophila melanogaster* strains. This work was supported by the list funding:

National Natural Science Foundation Key Project of China grant 91954114 (XH)
National Natural Science Foundation of China grant 32370799 (XH)
National Natural Science Foundation of China Youth Program grant 31801164 (ZQ) Natural Science Foundation of Shaanxi Province grant 2024JC-YBMS-638 (WH) Program of Innovative Research Team for the Central Universities grant GK202302003 (XH)

Additional information

Ethics Statement

All experiments were performed in accordance with the approved guidelines. The animal experiments were performed in accordance with the National Institute of Health's Guide for the Care and Use of Laboratory Animals and were approved by the Animal Care and Use Committee of Shaanxi normal university (Xi'an, China).

Author contributions

Conceptualization and experimental designing: XH, ZQ

Experiments performation: ZQ, MXY, XT, WAH, LFQ

Methodology and materials preparation: MXY, YL, WH, YQ

Data analysis and experimental advices: ZQ, LFQ, YL, WH

Writing - original draft: ZQ, XH

Writing - review & editing: ZQ, XH, WH

Funding acquisition: XH, ZQ, WH

Author ORCID iDs

Hui Xiao: https://orcid.org/0000-0001-9305-4486

Additional files

Data file S1. The screened proteins of LC-MS/MS preyed by Xkr-FLAG.

Data file S2. The screened proteins of LC-MS/MS preyed by Sac1-FLAG.

References

1. **Morioka S,** Kajioka D, Yamaoka Y, Ellison RM, Tufan T, Werkman IL, Tanaka S, Barron B, Ito ST, Kucenas S, *et al.* (2022) Chimeric efferocytic receptors improve apoptotic cell clearance and alleviate inflammation. *Cell* **185**:4887 https://doi.org/10.1016/j.cell.2022.11.029 | PubMed
2. **Brown GC** (2023) Cell death by phagocytosis. Nature Reviews Immunology.
3. **Birge RB,** Ucker DS (2008) Innate apoptotic immunity: the calming touch of death. *Cell Death and Differentiation* **15**:1096-1102 https://doi.org/10.1038/cdd.2008.58 | PubMed
4. **Segawa K,** Nagata S (2015) An Apoptotic 'Eat Me' Signal: Phosphatidylserine Exposure. *Trends in Cell Biology* **25**:639-650 https://doi.org/10.1016/j.tcb.2015.08.003 | PubMed
5. **Nagata S,** Hanayama R, Kawane K (2010) Autoimmunity and the Clearance of Dead Cells. *Cell* **140**:619-630 https://doi.org/10.1016/j.cell.2010.02.014 | PubMed

6. **Hankins HM,** Baldridge RD, Xu P, Graham TR (2015) Role of Flippases, Scramblases and Transfer Proteins in Phosphatidylserine Subcellular Distribution. *Traffic* **16**:35-47 https://doi.org/10.1111/tra.12233 | PubMed

7. **Suzuki J,** Imanishi E, Nagata S (2016) Xkr8 phospholipid scrambling complex in apoptotic phosphatidylserine exposure. *Proc Natl Acad Sci U S A* **113**:9509-9514 https://doi.org/10.1073/pnas.1610403113 | PubMed

8. **Kawano M,** Nagata S (2018) Lupus-like autoimmune disease caused by a lack of Xkr8, a caspase-dependent phospholipid scramblase. *Proc Natl Acad Sci U S A* **115**:2132-2137 https://doi.org/10.1073/pnas.1720732115 | PubMed

9. **Copic A,** Dieudonne T, Lenoir G (2023) Phosphatidylserine transport in cell life and death. *Curr Opin Cell Biol* **83**:102192 https://doi.org/10.1016/j.ceb.2023.102192 | PubMed

10. **Harayama T,** Riezman H (2018) Understanding the diversity of membrane lipid composition. *Nat Rev Mol Cell Biol* **19**:281-296 https://doi.org/10.1038/nrm.2017.138 | PubMed

11. **Wu H,** Carvalho P, Voeltz GK (2018) Here, there, and everywhere: The importance of ER membrane contact sites. *Science* **361** https://doi.org/10.1126/science.aan5835 | PubMed

12. **Cockcroft S,** Raghu P (2018) Phospholipid transport protein function at organelle contact sites. *Current Opinion in Cell Biology* **53**:52-60 https://doi.org/10.1016/j.ceb.2018.04.011 | PubMed

13. **Quon E,** Sere YY, Chauhan N, Johansen J, Sullivan DP, Dittman JS, Rice WJ, Chan RB, Di Paolo G, Beh CT, *et al.* (2018) Endoplasmic reticulum-plasma membrane contact sites integrate sterol and phospholipid regulation. *PLoS Biol* **16**:e2003864 https://doi.org/10.1371/journal.pbio.2003864 | PubMed

14. **Im YJ,** Raychaudhuri S, Prinz WA, Hurley JH (2005) Structural mechanism for sterol sensing and transport by OSBP-related proteins. *Nature* **437**:154-158 https://doi.org/10.1038/nature03923 | PubMed

15. **Du X,** Brown AJ, Yang H (2015) Novel mechanisms of intracellular cholesterol transport: oxysterol-binding proteins and membrane contact sites. *Curr Opin Cell Biol* **35**:37-42 https://doi.org/10.1016/j.ceb.2015.04.002 | PubMed

16. **Del Bel LM,** Brill JA (2018) Sac1, a lipid phosphatase at the interface of vesicular and nonvesicular transport. *Traffic* **19**:301-318 https://doi.org/10.1111/tra.12554 | PubMed

17. **Zheng Q,** Ma A, Yuan L, Gao N, Feng Q, Franc NC, Xiao H (2017) Apoptotic Cell Clearance in Drosophila melanogaster. *Front Immunol* **8**:1881 https://doi.org/10.3389/fimmu.2017.01881 | PubMed

18. **Kurant E,** Axelrod S, Leaman D, Gaul U (2008) Six-microns-under acts upstream of Draper in the glial phagocytosis of apoptotic neurons. *Cell* **133**:498-509 https://doi.org/10.1016/j.cell.2008.02.052 | PubMed

19. **Ziegenfuss JS,** Biswas R, Avery MA, Hong K, Sheehan AE, Yeung YG, Stanley ER, Freeman MR (2008) Draper-dependent glial phagocytic activity is mediated by Src and Syk family kinase signalling. *Nature* **453**:935-939 https://doi.org/10.1038/nature06901 | PubMed

20. **Ji H,** Wang B, Shen Y, Labib D, Lei J, Chen X, Sapar M, Boulanger A, Dura JM, Han C (2023) The Drosophila chemokine-like Orion bridges phosphatidylserine and Draper in phagocytosis of neurons. *Proc Natl Acad Sci U S A* **120**:e2303392120 https://doi.org/10.1073/pnas.2303392120 | PubMed

21. **Dolgikh A,** Rommelaere S, Ghanem A, Petrignani B, Poidevin M, Kurant E, Lemaitre B (2025) The secreted Nimrod protein NimB1 negatively regulates early steps of apoptotic cell phagocytosis in Drosophila. *Development* **152** https://doi.org/10.1242/dev.204919 | PubMed

22. **Armitage EL,** Roddie HG, Evans IR (2020) Overexposure to apoptosis via disrupted glial specification perturbs Drosophila macrophage function and reveals roles of the CNS during injury. *Cell Death Dis* **11**:627 https://doi.org/10.1038/s41419-020-02875-2 | PubMed

23. **Sapar ML,** Ji H, Wang B, Poe AR, Dubey K, Ren X, Ni JQ, Han C (2018) Phosphatidylserine Externalization Results from and Causes Neurite Degeneration in Drosophila. *Cell Rep* **24**:2273-2286 https://doi.org/10.1016/j.celrep.2018.07.095 | PubMed

24. **Evans IR,** Rodrigues FS, Armitage EL, Wood W (2015) Draper/CED-1 mediates an ancient damage response to control inflammatory blood cell migration in vivo. *Curr Biol* **25**:1606-1612 https://doi.org/10.1016/j.cub.2015.04.037 | PubMed

25. **Suzuki J,** Denning DP, Imanishi E, Horvitz HR, Nagata S (2013) Xk-related protein 8 and CED-8 promote phosphatidylserine exposure in apoptotic cells. *Science* **341**:403-406 https://doi.org/10.1126/science.1236758 | PubMed

26. **Shiomi A,** Nagao K, Yokota N, Tsuchiya M, Kato U, Juni N, Hara Y, Mori MX, Mori Y, Ui-Tei K, *et al.* (2021) Extreme deformability of insect cell membranes is governed by phospholipid scrambling. *Cell Rep* **35**:109219 https://doi.org/10.1016/j.celrep.2021.109219 | PubMed

27. **Chen YZ,** Mapes J, Lee ES, Skeen-Gaar RR, Xue D (2013) Caspase-mediated activation of Caenorhabditis elegans CED-8 promotes apoptosis and phosphatidylserine externalization. *Nat Commun* **4**:2726 https://doi.org/10.1038/ncomms3726 | PubMed

28. **Rogulja-Ortmann A,** Luer K, Seibert J, Rickert C, Technau GM (2007) Programmed cell death in the embryonic central nervous system of. *Development* **134**:105-116 https://doi.org/10.1242/dev.02707 | PubMed

29. **Cuttell L,** Vaughan A, Silva E, Escaron CJ, Lavine M, Van Goethem E, Eid JP, Quirin M, Franc NC (2008) Undertaker, a Junctophilin, Links Draper-Mediated Phagocytosis and Calcium Homeostasis. *Cell* **135**:524-534 https://doi.org/10.1016/j.cell.2008.08.033 | PubMed

30. **Zheng Q,** Gao N, Sun Q, Li X, Wang Y, Xiao H (2021) bfc, a novel serpent co-factor for the expression of croquemort, regulates efferocytosis in Drosophila melanogaster. *PLoS Genet* **17**:e1009947 https://doi.org/10.1371/journal.pgen.1009947 | PubMed

31. **Goto A,** Kadowaki T, Kitagawa Y (2003) hemolectin gene is expressed in embryonic and larval hemocytes and its knock down causes bleeding defects. *Developmental Biology* **264**:582-591 https://doi.org/10.1016/j.ydbio.2003.06.001 | PubMed

32. **Perrin J,** Mortier M, Jacomin AC, Viargues P, Thevenon D, Fauvarque MO (2015) The Nonaspanins TM9SF2 and TM9SF4 Regulate the Plasma Membrane Localization and Signalling Activity of the Peptidoglycan Recognition Protein PGRP-LC in. *J Innate Immun* **7**:37-46 https://doi.org/10.1159/000365112 | PubMed

33. **Lozupone F,** Borghi M, Marzoli F, Azzarito T, Matarrese P, lessi E, Venturi G, Meschini S, Canitano A, Bona R, *et al.* (2015) TM9SF4 is a novel V-ATPase-interacting protein that modulates tumor pH alterations associated with drug resistance and invasiveness of colon cancer cells. *Oncogene* **34**:5163-5174 https://doi.org/10.1038/onc.2014.437 | PubMed

34. **Bergeret E,** Perrin J, Williams M, Grunwald D, Engel E, Thevenon D, Taillebourg E, Bruckert F, Cosson P, Fauvarque MO (2008) TM9SF4 is required for cellular immunity via cell adhesion and phagocytosis. *Journal of Cell Science* **121**:3325-3334 https://doi.org/10.1242/jcs.030163 | PubMed

35. **Hein MY,** Hubner NC, Poser I, Cox J, Nagaraj N, Toyoda Y, Gak IA, Weisswange I, Mansfeld J, Buchholz F, *et al.* (2015) A Human Interactome in Three Quantitative Dimensions Organized by Stoichiometries and Abundances. *Cell* **163**:712-723 https://doi.org/10.1016/j.cell.2015.09.053 | PubMed

36. **Yeung T,** Gilbert GE, Shi J, Silvius J, Kapus A, Grinstein S (2008) Membrane phosphatidylserine regulates surface charge and protein localization. *Science* **319**:210-213 https://doi.org/10.1126/science.1152066 | PubMed

37. **Maeda K,** Anand K, Chiapparino A, Kumar A, Poletto M, Kaksonen M, Gavin AC (2013) Interactome map uncovers phosphatidylserine transport by oxysterol-binding proteins. *Nature* **501**:257-261 https://doi.org/10.1038/nature12430 | PubMed

38. **Chung J,** Torta F, Masai K, Lucast L, Czapla H, Tanner LB, Narayanaswamy P, Wenk MR, Nakatsu F, De Camilli P (2015) INTRACELLULAR TRANSPORT. PI4P/phosphatidylserine countertransport at ORP5- and ORP8-mediated ER-plasma membrane contacts. *Science* **349**:428-432 https://doi.org/10.1126/science.aab1370 | PubMed

39. **Pemberton JG,** Kim YJ, Balla T (2020) Integrated regulation of the phosphatidylinositol cycle and phosphoinositide-driven lipid transport at ER-PM contact sites. *Traffic* **21**:200-219 https://doi.org/10.1111/tra.12709 | PubMed

40. **Phillips MJ,** Voeltz GK (2016) Structure and function of ER membrane contact sites with other organelles. *Nat Rev Mol Cell Biol* **17**:69-82 https://doi.org/10.1038/nrm.2015.8 | PubMed

41. **Chang CL,** Hsieh TS, Yang TT, Rothberg KG, Azizoglu DB, Volk E, Liao JC, Liou J (2013) Feedback Regulation of Receptor-Induced Ca2+ Signaling Mediated by E-Syt1 and Nir2 at Endoplasmic Reticulum-Plasma Membrane Junctions. *Cell Rep* **5**:813-825 https://doi.org/10.1016/j.celrep.2013.09.038 | PubMed

42. **Sakuragi T,** Kosako H, Nagata S (2019) Phosphorylation-mediated activation of mouse Xkr8 scramblase for phosphatidylserine exposure. *P Natl Acad Sci USA* **116**:2907-2912 https://doi.org/10.1073/pnas.1820499116 | PubMed

43. **Raschke WC,** Baird S, Ralph P, Nakoinz I (1978) Functional macrophage cell lines transformed by Abelson leukemia virus. *Cell* **15**:261-267 https://doi.org/10.1016/0092-8674(78)90101-0 | PubMed

44. **Nishi C,** Yanagihashi Y, Segawa K, Nagata S (2019) MERTK tyrosine kinase receptor together with TIM4 phosphatidylserine receptor mediates distinct signal transduction pathways for efferocytosis and cell proliferation. *J Biol Chem* **294**:7221-7230 https://doi.org/10.1074/jbc.ra118.006628 | PubMed

45. **Mapes J,** Chen YZ, Kim A, Mitani S, Kang BH, Xue D (2012) CED-1, CED-7, and TTR-52 regulate surface phosphatidylserine expression on apoptotic and phagocytic cells. *Curr Biol* **22**:1267-1275 https://doi.org/10.1016/j.cub.2012.05.052 | PubMed

46. **Ji H,** Wang B, Shen YF, Labib D, Lei J, Chen XC, Sapar M, Boulanger A, Dura JM, Han C (2023) The chemokine-like Orion bridges phosphatidylserine and Draper in phagocytosis of neurons. *P Natl Acad Sci USA* **120** https://doi.org/10.1073/pnas.2303392120 | PubMed

47. **Fais S,** Fauvarque MO (2012) TM9 and cannibalism: how to learn more about cancer by studying amoebae and invertebrates. *Trends Mol Med* **18**:4-5 https://doi.org/10.1016/j.molmed.2011.09.001 | PubMed

48. **Ghai R,** Du X, Wang H, Dong J, Ferguson C, Brown AJ, Parton RG, Wu JW, Yang H (2017) ORP5 and ORP8 bind phosphatidylinositol-4, 5-biphosphate (PtdIns(4,5)P (2)) and regulate its level at the plasma membrane. *Nat Commun* **8**:757 https://doi.org/10.1038/s41467-017-00861-5 | PubMed

49. **D'Ambrosio JM,** Albanese V, Lipp NF, Fleuriot L, Debayle D, Drin G, Copic A (2020) Osh6 requires Ist2 for localization to ER-PM contacts and efficient phosphatidylserine transport in budding yeast. *J Cell Sci* **133**:jcs243733 https://doi.org/10.1242/jcs.243733 | PubMed

50. **Moser von Filseck J,** Copic A, Delfosse V, Vanni S, Jackson CL, Bourguet W, Drin G (2015) INTRACELLULAR TRANSPORT. Phosphatidylserine transport by ORP/Osh proteins is driven by phosphatidylinositol 4-phosphate. *Science* **349**:432-436 https://doi.org/10.1126/science.aab1346 | PubMed

51. **Mesmin B,** Bigay J, Moser von Filseck J, Lacas-Gervais S, Drin G, Antonny B (2013) A four-step cycle driven by PI(4)P hydrolysis directs sterol/PI(4)P exchange by the ER-Golgi tether OSBP. *Cell* **155**:830-843 https://doi.org/10.1016/j.cell.2013.09.056 | PubMed

52. **Sohn M,** Korzeniowski M, Zewe JP, Wills RC, Hammond GRV, Humpolickova J, Vrzal L, Chalupska D, Veverka V, Fairn GD, *et al.* (2018) PI(4,5)P(2) controls plasma membrane PI4P and PS levels via ORP5/8 recruitment to ER-PM contact sites. *J Cell Biol* **217**:1797-1813 https://doi.org/10.1083/jcb.201710095 | PubMed

53. **He R,** Liu F, Wang H, Huang S, Xu K, Zhang C, Liu Y, Yu H (2023) ORP9 and ORP10 form a heterocomplex to transfer phosphatidylinositol 4-phosphate at ER-TGN contact sites. *Cell Mol Life Sci* **80**:77 https://doi.org/10.1007/s00018-023-04728-5 | PubMed

54. **Kawasaki A,** Sakai A, Nakanishi H, Hasegawa J, Taguchi T, Sasaki J, Arai H, Sasaki T, Igarashi M, Nakatsu F (2022) PI4P/PS countertransport by ORP10 at ER-endosome membrane contact sites regulates endosome fission. *J Cell Biol* **221** https://doi.org/10.1083/jcb.202103141 | PubMed

55. **Tan JX,** Finkel T (2022) A phosphoinositide signalling pathway mediates rapid lysosomal repair. *Nature* **609**:815-821 https://doi.org/10.1038/s41586-022-05164-4 | PubMed

56. **Naito T,** Yang H, Koh DHZ, Mahajan D, Lu L, Saheki Y (2023) Regulation of cellular cholesterol distribution via non-vesicular lipid transport at ER-Golgi contact sites. *Nat Commun* **14**:5867 https://doi.org/10.1038/s41467-023-41213-w | PubMed

57. **Ryoden Y,** Nagata S (2022) The XK plasma membrane scramblase and the VPS13A cytosolic lipid transporter for ATP-induced cell death. *Bioessays* **44**:e2200106 https://doi.org/10.1002/bies.202200106 | PubMed

58. **Han K** (1996) An efficient DDAB-mediated transfection of Drosophila S2 cells. *Nucleic Acids Res* **24**:4362-4363 https://doi.org/10.1093/nar/24.21.4362 | PubMed

59. **Fairn GD,** Schieber NL, Ariotti N, Murphy S, Kuerschner L, Webb RI, Grinstein S, Parton RG (2011) High-resolution mapping reveals topologically distinct cellular pools of phosphatidylserine. *J Cell Biol* **194**:257-275 https://doi.org/10.1083/jcb.201012028 | PubMed

60. **Luik RM,** Wang B, Prakriya M, Wu MM, Lewis RS (2008) Oligomerization of STIM1 couples ER calcium depletion to CRAC channel activation. *Nature* **454**:538-U511 https://doi.org/10.1038/nature07065 | PubMed

61. **Heo WD,** Inoue T, Park WS, Kim ML, Park BO, Wandless TJ, Meyer T (2006) PI(3,4,5)P and PI(4,5)P lipids target proteins with polybasic clusters to the plasma membrane. *Science* **314**:1458-1461 https://doi.org/10.1126/science.1134389 | PubMed

62. **Yamashita Y,** Suzuki C, Uchiyama Y, Nagata S (2020) Infertility Caused by Inefficient Apoptotic Germ Cell Clearance in Xkr8-Deficient Male Mice. *Mol Cell Biol* **40** https://doi.org/10.1128/mcb.00402-19 | PubMed

63. **Nagano M,** Ui-Tei K, Suzuki H, Piao Z, Miyata Y (2000) CDK inhibitors suppress apoptosis induced by chemicals and by excessive expression of a cell death gene, reaper, in Drosophila cells. *Apoptosis* **5**:543-550 https://doi.org/10.1023/a:1009641613826 | PubMed

64. **Bassett AR,** Tibbit C, Ponting CP, Liu JL (2014) Mutagenesis and homologous recombination in Drosophila cell lines using CRISPR/Cas9. *Biol Open* **3**:42-49 https://doi.org/10.1242/bio.20137120 | PubMed

65. **Obrdlik P,** El-Bakkoury M, Hamacher T, Cappellaro C, Vilarino C, Fleischer C, Ellerbrok H, Kamuzinzi R, Ledent V, Blaudez D, *et al.* (2004) K+ channel interactions detected by a genetic system optimized for systematic studies of membrane protein interactions. In: *Proceedings of the National Academy of Sciences of the United States of America* Proceedings of the National Academy of Sciences of the United States of America. **101** pp. 12242-12247 https://doi.org/10.1073/pnas.0404467101 | PubMed

66. **Gookin TE,** Assmann SM (2014) Significant reduction of BiFC non-specific assembly facilitates in planta assessment of heterotrimeric G-protein interactors. *Plant J* **80**:553-567 https://doi.org/10.1111/tpj.12639 | PubMed

67. **Shlyakhover E,** Shklyar B, Hakim-Mishnaevski K, Levy-Adam F, Kurant E (2018) Drosophila GATA Factor Serpent Establishes Phagocytic Ability of Embryonic Macrophages. *Front Immunol* **9**:266 https://doi.org/10.3389/fimmu.2018.00266 | PubMed

68. **Silva E,** Au-Yeung HW, Van Goethem E, Burden J, Franc NC (2007) Requirement for a Drosophila E3-ubiquitin ligase in phagocytosis of apoptotic cells. *Immunity* **27**:585-596 https://doi.org/10.1016/j.immuni.2007.08.016 | PubMed

69. **Gao N,** Zheng Q, Wang YZ, Li XW, Li Z, Xiao H (2022) Wun2-mediated integrin recycling promotes apoptotic cell clearance in Drosophila. *Cell Death and Differentiation* **29**:2545-2561 https://doi.org/10.1038/s41418-022-01039-3 | PubMed

70. **Abramson J,** Adler J, Dunger J, Evans R, Green T, Pritzel A, Ronneberger O, Willmore L, Ballard AJ, Bambrick J, *et al.* (2024) Accurate structure prediction of biomolecular interactions with AlphaFold 3. *Nature* **630**:493-500 https://doi.org/10.1038/s41586-024-07487-w | PubMed

71. **Stepczynska A,** Lauber K, Engels IH, Janssen O, Kabelitz D, Wesselborg S, Schulze-Osthoff K (2001) Staurosporine and conventional anticancer drugs induce overlapping, yet distinct pathways of apoptosis and caspase activation. *Oncogene* **20**:1193-1202 https://doi.org/10.1038/sj.onc.1204221 | PubMed

72. **Perez-Riverol Y,** Bai J, Bandla C, Garcia-Seisdedos D, Hewapathirana S, Kamatchinathan S, Kundu DJ, Prakash A, Frericks-Zipper A, Eisenacher M, *et al.* (2022) The PRIDE database resources in 2022: a hub for mass spectrometry-based proteomics evidences. *Nucleic Acids Res* **50**:D543-D552 https://doi.org/10.1093/nar/gkab1038 | PubMed

Xiao Hui (2024) Drosophila melanogaster Xkr interacting proteins shotgun LC-MS/MS data. PRIDE. ID PXD058895 https://www.ebi.ac.uk/pride/archive/projects/PXD058895

Peer reviews

Reviewer #1 (Public review):

Summary:

The authors characterize the phospholipid scramblase Xkr in Drosophila. They generate null mutants in both S2 cells and flies and find that phosphatidylserine (PS) exposure is reduced during apoptosis; they show reduced engulfment of apoptotic cells, and that the protein is localized partially within the cytoplasm, overlapping with the ER. They go on to identify Xkr binding partners and show that they overlap with plasma membrane-ER contact sites, suggesting that Xkr facilitates PS transfer from the ER to PM. Overall, this reveals a new role for Xkr and identifies new binding partners, which are valuable contributions to the field.

Strengths:

(1) The generation of new Xkr reagents in both S2 cells and flies to analyze its function. Tools are used to quantify both PS exposure and efferocytosis, and the effects of Xkr knockout are significant.

(2) The discovery of new binding partners of Xkr which also affect PS exposure and efferocytosis.

(3) The authors demonstrate that the binding partners are conserved in mammalian cells.

Weaknesses:

(1) Throughout the manuscript (e.g, lines 105, 165, 274 and discussion), the authors describe Xkr as being activated in a caspase-independent manner, and use this as the rationale for identifying binding partners. However, this is never shown in the manuscript or clearly referenced. Interestingly, there is a TEVDA sequence in the fly ortholog at the same location as the caspase cleavage site in C. elegans Ced-8 (Figure S1), suggesting the caspase cleavage site is conserved. This should be further investigated, or the statements regarding caspase independence should be modified. I don't think the N- and C-terminal GFP fusions indicate caspase independence, especially since apoptosis was not induced in Figure 1A, B. If cleavage occurred at the TEVDA site in Figure S1A, it would not lead to a noticeable change on the Western blot, although the size does look a bit smaller in Figure S2B at the 8 h time point.

(2) The authors examine overlap between tagged Xkr and cellular compartment markers and find substantial overlap with Lamp (and other vesicle markers to a lesser extent) (Figure S2). This is not addressed in the paper and could indicate engulfment of other cells since S2 cells are macrophages. To test this, the staining could be tested on the mixed cells (vesicle-GFP tagged S2 + apoptotic xkr-mcherry). Similarly, calreticulin is an eatme signal that gets translocated to the PM of apoptotic cells. This could affect interpretation of colocalization (Figure 2J), and ideally another ER marker should be used.

(3) There are some places where there is over- or incorrect interpretation, and these instances should be corrected.

Specific examples:

a) Line 342 "Relative expression analysis by RT-qPCR showed that all three mutants were likely null alleles." This does not make sense since there is still mRNA present. In Figure S7A, the tm9sf4 allele is expressed at 75% of the control. The others show a greater reduction, but this is not proof of a null allele.

b) Figure S3I - It looks like mCherry-Lact:C2 does get localized to the PM with AcD treatment in the xkr[ko], although the authors conclude "this disrupted PS localization to the PM could not be restored by apoptosis induction". However, the PM localization does look disrupted in the tm9sf4 and sac1 knockdowns.

c) Figure 3I. The control Lact:C2 staining looks very different from the staining in Figure 2J, with abundant Lact:C2 outside the cell. Given the variability in the staining, were the contact sites quantified? On lines 287-288, it is stated that "fewer ER-PM MCSs were detected in xkrko cells than in WT", but no quantification is provided.

d) Line 299-300 - "the interaction between Xkr and dORP9 was enhanced after apoptosis induction". The interaction does not look enhanced in Figure S5F, so this statement should be removed or data supporting the statement should be provided. The interaction between Xkr and dORP2 looks enhanced upon apoptosis induction, but also paradoxically looks even more enhanced when apoptosis is blocked.

e) The data in Figure S6 are highlighted in the abstract. If this is a major conclusion, it would be best to move it to the main text and provide quantification.

f) Lines 392-4. The concluding statement seems overstated given that there was only a modest inhibition of PS exposure in the osbpl5 knockdown (Figure 6A) and no defects in efferocytosis (Figure 6C). The osbpl8 showed a stronger effect on PS exposure but still a very modest effect on efferocytosis.

https://doi.org/10.7554/eLife.112294.1.sa2

Reviewer #2 (Public review):

In this study, the authors investigate the mechanisms underlying phosphatidylserine (PS) exposure during efferocytosis in Drosophila. They first show that Xkr promotes PS exposure and apoptotic cell clearance in both S2 cells and Drosophila embryos. As Drosophila Xkr lacks the canonical caspase cleavage site found in mammalian XKR proteins, the authors further explore the underlying mechanism by which Xkr regulates PS externalization. Through protein interaction studies, they identify TM9SF4 as an interacting partner of Xkr that regulates PS distribution and show that non-vesicular PS transport contributes to apoptotic PS exposure and efferocytosis. Using protein interaction studies, they further demonstrate that Xkr interacts with the lipid transfer protein dORP9 at ER-PM contact sites to facilitate non-vesicular PS transport to the plasma membrane. Loss of these proteins affects PS externalization and efferocytosis in Drosophila. Finally, using human cells, they demonstrate that human OSBPL8 interacts with XKR8 to regulate apoptotic PS exposure. Overall, the study supports a model in which Xkr promotes efferocytosis by facilitating lipid transport in addition to its role as a phospholipid scramblase.

https://doi.org/10.7554/eLife.112294.1.sa1

Reviewer #3 (Public review):

Summary:

The manuscript investigates the function of the Drosophila Xkr protein, a homolog of mammalian Xkr8 that lacks the canonical caspase-cleavage motif. The authors show that apoptotic stimuli increase Xkr protein abundance through a post-transcriptional mechanism and that Xkr promotes phosphatidylserine (PS) exposure during apoptosis. Using immunoprecipitation coupled with mass spectrometry, they identify TM9SF4 as an Xkr-interacting protein and further implicate TM9SF4, Sac1, dORP2, dORP9, and Vap33 in regulating apoptotic PS exposure and efferocytosis. Based on these findings, the authors propose that Xkr regulates PS transport at ER-PM contact sites. Similar observations are also presented in human cells.

Strengths:

Overall, this is an interesting study. The authors provide convincing evidence that Drosophila Xkr participates in apoptotic PS exposure and employ multiple complementary approaches to support the involvement of several proteins in this pathway. The identification of TM9SF4 as a potential regulator of Xkr-mediated PS exposure is likely to be of broad interest.

Weaknesses:

I am less convinced by the evidence supporting the proposed role of ER-PM contact sites, and several mechanistic conclusions appear to extend beyond the data presented. Addressing the following points would substantially strengthen the manuscript.

Major concerns:

(1) In Figure 2A and related text, it is unclear whether the mass spectrometry analysis was performed using untreated cells or AcD-treated cells. If the objective was to identify apoptosis-associated Xkr interactors, it would be helpful to clarify the experimental condition and explain whether apoptosis-specific interactors were analyzed separately.

(2) In Figure 2B, 2E, and several other co-IP results, a negative control of Flag tag only is required to exclude experimental errors like insufficient washing, etc.

(3) In Figure S3B, S3F, and several other BiFC results, an mVC-only negative control would be important to exclude nonspecific fluorescence complementation.

(4) In Figure 2G, the quantitative values appear inconsistent with the flow cytometry histograms. The peak shift following Sac1 knockdown appears smaller than that of TM9SF4 knockdown, whereas the quantified values suggest the opposite. Please clarify this apparent discrepancy.

(5) I find the interpretation in Lines 223-227 difficult to reconcile with the data. Knockdown of both tm9sf4 and sac1 impaired apoptotic PS exposure to a similar extent as xkr knockout. However, while xkr deficiency significantly reduced efferocytosis, sac1 knockdown produced only a modest, statistically insignificant effect. These observations suggest that impaired PS exposure alone may not fully account for the efferocytosis phenotype observed in xkr-deficient cells. These results appear difficult to reconcile with the proposed model, which needs careful discussion.

(6) In Lines 274-275, the authors state that 'increased Xkr may accelerate non-vesicular PS transport for efficient apoptotic PS exposure'. However, Xkr protein levels increase only ~8 h after AcD treatment, whereas PS exposure occurs much earlier. Thus, alternative explanations like Xkr relocalization (Figure S5C), rather than increased abundance, may also

explain how Xkr mediates PS transport. An Xkr overexpression experiment could be helpful to support this statement.

(7) The interpretation of the MAPPER experiments requires further clarification. In Line 283, the authors refer to "the intracellular proportion of the signal for each protein overlapping with MAPPER." Since MAPPER is designed to label ER-PM contact sites, which are located on the plasma membrane, intracellular MAPPER fluorescence likely represents the ER network rather than bona fide ER-PM contacts. Throughout the manuscript (including Figure S6, etc.), intracellular MAPPER puncta appear to be interpreted as ER-PM contacts, which may not be appropriate. In contrast, the peripheral MAPPER puncta observed along the cell cortex (e.g., Figure S5C after AcD treatment) are more consistent with authentic ER-PM contact sites. It is also not obvious that these cortical MAPPER signals colocalize with Xkr(Figure S5C). Thus, while the data support a role for the ER, they do not yet convincingly demonstrate Xkr clustering at ER-PM contact sites.

(8) In the Xkr knockout cells, all fluorescence signals appear substantially low in intensity. Differences in protein distribution are difficult to interpret when overall probe expression also appears altered. It would be helpful to demonstrate that probe expression levels are comparable between conditions. Furthermore, as noted above, intracellular MAPPER signal may primarily represent ER rather than ER-PM contacts. Finally, despite the reduced signal intensity, the remaining MAPPER and PS signals still appear well colocalized in the knockout cells, similar to the observations in Figure 2J. The interpretation in Lines 285-288 should therefore be reconsidered.

https://doi.org/10.7554/eLife.112294.1.sa0

Author response:

Public Reviews:

Reviewer #1 (Public review):

Summary:

The authors characterize the phospholipid scramblase Xkr in Drosophila. They generate null mutants in both S2 cells and flies and find that phosphatidylserine (PS) exposure is reduced during apoptosis; they show reduced engulfment of apoptotic cells, and that the protein is localized partially within the cytoplasm, overlapping with the ER. They go on to identify Xkr binding partners and show that they overlap with plasma membrane-ER contact sites, suggesting that Xkr facilitates PS transfer from the ER to PM. Overall, this reveals a new role for Xkr and identifies new binding partners, which are valuable contributions to the field.

Strengths:

(1) The generation of new Xkr reagents in both S2 cells and flies to analyze its function. Tools are used to quantify both PS exposure and efferocytosis, and the effects of Xkr knockout are significant.

(2) The discovery of new binding partners of Xkr which also affect PS exposure and efferocytosis.

(3) The authors demonstrate that the binding partners are conserved in mammalian cells.

Weaknesses:

> *(1) Throughout the manuscript (e.g, lines 105, 165, 274 and discussion), the authors describe Xkr as being activated in a caspase-independent manner, and use this as the rationale for identifying binding partners. However, this is never shown in the manuscript or clearly referenced. Interestingly, there is a TEVDA sequence in the fly ortholog at the same location as the caspase cleavage site in C. elegans Ced-8 (Figure S1), suggesting the caspase cleavage site is conserved. This should be further investigated, or the statements regarding caspase independence should be modified. I don't think the N- and C-terminal GFP fusions indicate caspase independence, especially since apoptosis was not induced in Figure 1A, B. If cleavage occurred at the TEVDA site in Figure S1A, it would not lead to a noticeable change on the Western blot, although the size does look a bit smaller in Figure S2B at the 8 h time point.*

We thank the reviewer for pointing out that, as E/DXXD has been considered a conserved caspase-3 cleavage site, TEVDA has also been validated as a caspase-6 cleavage site, which we have missed. We will further confirm this using site-mutated expression vectors in S2 cells.

> *(2) The authors examine overlap between tagged Xkr and cellular compartment markers and find substantial overlap with Lamp (and other vesicle markers to a lesser extent) (Figure S2). This is not addressed in the paper and could indicate engulfment of other cells since S2 cells are macrophages. To test this, the staining could be tested on the mixed cells (vesicle-GFP tagged S2 + apoptotic xkr-mcherry). Similarly, calreticulin is an eatme signal that gets translocated to the PM of apoptotic cells. This could affect interpretation of colocalization (Figure 2J), and ideally another ER marker should be used.*

We thank the reviewer for the suggestion. We will attempt to label Xkr-mCherry under apoptosis with other vesicles and change the ER marker to Cnx99A (Calnexin ortholog in Drosophila).

> *(3) There are some places where there is over- or incorrect interpretation, and these instances should be corrected.*

We thank the reviewer for their careful reading, and we will correct the mistakes in the revised manuscript.

> *Specific examples:*
>
> *a) Line 342 "Relative expression analysis by RT-qPCR showed that all three mutants were likely null alleles." This does not make sense since there is still mRNA present. In Figure S7A, the tm9sf4 allele is expressed at 75% of the control. The others show a greater reduction, but this is not proof of a null allele.*

We agree with the reviewer's opinion. These mutants from the BDSC are not completely deleted but partially deleted; therefore, the RT-qPCR assay may not be very accurate. We will detect the mRNA levels of *tm9sf4*, *dorp9*, and *sac1* using RT primers from different cDNA regions to make the results more convincing.

> *b) Figure S3I - It looks like mCherry-Lact:C2 does get localized to the PM with AcD treatment in the xkr[ko], although the authors conclude "this disrupted PS localization to the PM could not be restored by apoptosis induction". However, the PM localization does look disrupted in the tm9sf4 and sac1 knockdowns.*

We thank you for raising this intriguing hypothesis. Indeed, PM localization of Lact:C2 was reduced in xkr^{ko} cells, and the distribution could not be rescued after apoptosis. Unlike xkr^{ko}, *tm9sf4*, and *sac1* RNAi-treated cells displayed weak PS disorder, which may be due to the

efficiency of knockdown. However, the statistical results indicated that the ratio of PM/Cyto was reduced in *tm9sf4* and *sac1* RNAi-treated cells.

> *c) Figure 3I. The control Lact:C2 staining looks very different from the staining in Figure 2J, with abundant Lact:C2 outside the cell. Given the variability in the staining, were the contact sites quantified? On lines 287-288, it is stated that "fewer ER-PM MCSs were detected in xkrko cells than in WT", but no quantification is provided.*

We thank for the reviewer's suggestion. We will add the statistical results of Fig. 3I in the revised version.

> *d) Line 299-300 - "the interaction between Xkr and dORP9 was enhanced after apoptosis induction". The interaction does not look enhanced in Figure S5F, so this statement should be removed or data supporting the statement should be provided. The interaction between Xkr and dORP2 looks enhanced upon apoptosis induction, but also paradoxically looks even more enhanced when apoptosis is blocked.*

We thank you for raising this intriguing hypothesis. We will delete the relevant statement to eliminate unnecessary misunderstandings.

> *e) The data in Figure S6 are highlighted in the abstract. If this is a major conclusion, it would be best to move it to the main text and provide quantification.*

We thank for the reviewer's suggestion. We will move this to the main text and provide quantification in the revised version.

> *f) Lines 392-4. The concluding statement seems overstated given that there was only a modest inhibition of PS exposure in the osbpl5 knockdown (Figure 6A) and no defects in efferocytosis (Figure 6C). The osbpl8 showed a stronger effect on PS exposure but still a very modest effect on efferocytosis.*

We thank for the reviewer's suggestion. We will weaken the statement in the Results section of Figure 6 and perform *osbpl9* knockdown to observe efferocytosis in Raw264.7 cells, as OSBPL9 interacts with Xkr8 strongly.

> ***Reviewer #2 (Public review):***
>
> *In this study, the authors investigate the mechanisms underlying phosphatidylserine (PS) exposure during efferocytosis in Drosophila. They first show that Xkr promotes PS exposure and apoptotic cell clearance in both S2 cells and Drosophila embryos. As Drosophila Xkr lacks the canonical caspase cleavage site found in mammalian XKR proteins, the authors further explore the underlying mechanism by which Xkr regulates PS externalization. Through protein interaction studies, they identify TM9SF4 as an interacting partner of Xkr that regulates PS distribution and show that non-vesicular PS transport contributes to apoptotic PS exposure and efferocytosis. Using protein interaction studies, they further demonstrate that Xkr interacts with the lipid transfer protein dORP9 at ER-PM contact sites to facilitate non-vesicular PS transport to the plasma membrane. Loss of these proteins affects PS externalization and efferocytosis in Drosophila. Finally, using human cells, they demonstrate that human OSBPL8 interacts with XKR8 to regulate apoptotic PS exposure. Overall, the study supports a model in which Xkr promotes efferocytosis by facilitating lipid transport in addition to its role as a phospholipid scramblase.*

Thank you for your comprehensive and generous assessment of our work and for the time and expertise you have devoted to reviewing our manuscript. We will revise the manuscript accordingly and provide a point-by-point response in the revised version.

> ***Reviewer #3 (Public review):***
>
> *Summary:*
>
> *The manuscript investigates the function of the Drosophila Xkr protein, a homolog of mammalian Xkr8 that lacks the canonical caspase-cleavage motif. The authors show that apoptotic stimuli increase Xkr protein abundance through a post-transcriptional mechanism and that Xkr promotes phosphatidylserine (PS) exposure during apoptosis. Using immunoprecipitation coupled with mass spectrometry, they identify TM9SF4 as an Xkr-interacting protein and further implicate TM9SF4, Sac1, dORP2, dORP9, and Vap33 in regulating apoptotic PS exposure and efferocytosis. Based on these findings, the authors propose that Xkr regulates PS transport at ER-PM contact sites. Similar observations are also presented in human cells.*
>
> *Strengths:*
>
> *Overall, this is an interesting study. The authors provide convincing evidence that Drosophila Xkr participates in apoptotic PS exposure and employ multiple complementary approaches to support the involvement of several proteins in this pathway. The identification of TM9SF4 as a potential regulator of Xkr-mediated PS exposure is likely to be of broad interest.*
>
> *Weaknesses:*
>
> *I am less convinced by the evidence supporting the proposed role of ER-PM contact sites, and several mechanistic conclusions appear to extend beyond the data presented. Addressing the following points would substantially strengthen the manuscript.*

We sincerely thank you for your careful reading and accurate summary of our manuscript. We appreciate the time, effort, and expertise you have dedicated to evaluating our work, and we will try our best to improve our manuscript according to your suggestions.

> *Major concerns:*
>
> *(1) In Figure 2A and related text, it is unclear whether the mass spectrometry analysis was performed using untreated cells or AcD-treated cells. If the objective was to identify apoptosis-associated Xkr interactors, it would be helpful to clarify the experimental condition and explain whether apoptosis-specific interactors were analyzed separately.*

We thank for the reviewer's suggestion. We used AcD-treated S2 cells and untreated S2 cells to perform mass spectrometry. To clarify this, we will add a detailed method description in the method section.

> *(2) In Figure 2B, 2E, and several other co-IP results, a negative control of Flag tag only is required to exclude experimental errors like insufficient washing, etc.*

We thank for the reviewer's suggestion. We used anti-HA magnetic beads to perform immunoprecipitation, and single HA-TM9SF4 was used as a negative control.

> *(3) In Figure S3B, S3F, and several other BiFC results, an mVC-only negative control would be important to exclude nonspecific fluorescence complementation.*

We thank for the reviewer's suggestion, we will add the negative control for BiFC results in the revised version.

> *(4) In Figure 2G, the quantitative values appear inconsistent with the flow cytometry histograms. The peak shift following Sac1 knockdown appears smaller than that of*

> *TM9SF4 knockdown, whereas the quantified values suggest the opposite. Please clarify this apparent discrepancy.*

We sincerely thank you for the careful consideration of our statistical results, which were obtained from 3 repeats. We will choose another flow cytometry histogram of tm9sf4 and sac1 to make the data and images more consistent.

> *(5) I find the interpretation in Lines 223-227 difficult to reconcile with the data. Knockdown of both tm9sf4 and sac1 impaired apoptotic PS exposure to a similar extent as xkr knockout. However, while xkr deficiency significantly reduced efferocytosis, sac1 knockdown produced only a modest, statistically insignificant effect. These observations suggest that impaired PS exposure alone may not fully account for the efferocytosis phenotype observed in xkr-deficient cells. These results appear difficult to reconcile with the proposed model, which needs careful discussion.*

We sincerely thank the reviewer for their careful and thoughtful observations. Given the results we have observed, we will add this to the discussion section in the revised version.

> *(6) In Lines 274-275, the authors state that 'increased Xkr may accelerate non-vesicular PS transport for efficient apoptotic PS exposure'. However, Xkr protein levels increase only ~8 h after AcD treatment, whereas PS exposure occurs much earlier. Thus, alternative explanations like Xkr relocalization (Figure S5C), rather than increased abundance, may also explain how Xkr mediates PS transport. An Xkr overexpression experiment could be helpful to support this statement.*

We thank for the reviewer's suggestion. We will overexpress Xkr with or without AcD treatment to observe whether the localization or amount of Lact:C2 changes and to re-evaluate the role of Xkr in PS exposure.

> *(7) The interpretation of the MAPPER experiments requires further clarification. In Line 283, the authors refer to "the intracellular proportion of the signal for each protein overlapping with MAPPER." Since MAPPER is designed to label ER-PM contact sites, which are located on the plasma membrane, intracellular MAPPER fluorescence likely represents the ER network rather than bona fide ER-PM contacts. Throughout the manuscript (including Figure S6, etc.), intracellular MAPPER puncta appear to be interpreted as ER-PM contacts, which may not be appropriate. In contrast, the peripheral MAPPER puncta observed along the cell cortex (e.g., Figure S5C after AcD treatment) are more consistent with authentic ER-PM contact sites. It is also not obvious that these cortical MAPPER signals colocalize with Xkr(Figure S5C). Thus, while the data support a role for the ER, they do not yet convincingly demonstrate Xkr clustering at ER-PM contact sites.*

We thank the reviewer for the suggestion, and we believe that the TIRF technique can help us demonstrate the ER-PM signal. Since our college has no TIRF microscope, we will try our best to seek cooperation from other colleges to achieve this experiment.

> *(8) In the Xkr knockout cells, all fluorescence signals appear substantially low in intensity. Differences in protein distribution are difficult to interpret when overall probe expression also appears altered. It would be helpful to demonstrate that probe expression levels are comparable between conditions. Furthermore, as noted above, intracellular MAPPER signal may primarily represent ER rather than ER-PM contacts. Finally, despite the reduced signal intensity, the remaining MAPPER and PS signals still appear well colocalized in the knockout cells, similar to the observations in Figure 2J. The interpretation in Lines 285-288 should therefore be reconsidered.*

We sincerely thank the reviewer for this careful and thoughtful observation, and we agree that the interpretation in Line 285-288 is overstated. To explain this, we plan to detect the

Lact:C2 and MAPPER signals in S2 and xkr^{ko} cells with or without AcD to confirm how Xkr regulates PS via ER-PM under apoptotic conditions.

https://doi.org/10.7554/eLife.112294.1.sa4